Electronic Supplementary Material (ESI) for Polymer Chemistry.

(Supporting Information)

Helicity Induction and Memory Effect in Poly(biphenylylacetylene)s Bearing Various Functional Groups and Their Use as Switchable Chiral Stationary Phases for HPLC

Ryoma Ishidate,[1,2] Toru Sato,[1] Tomoyuki Ikai,[1,2] Shigeyoshi Kanoh,[1] Eiji Yashima*[2] and Katsuhiro Maeda*[1,3]

[1]Graduate School of Natural Science and Technology, Kanazawa University, Kakuma-machi, Kanazawa 920-1192, Japan, [2]Department of Molecular Design and Engineering, Graduate School of Engineering, Nagoya University, Chikusa-ku, Nagoya 464-8603, Japan, [3]Nano Life Science Institute (WPI-NanoLSI), Kanazawa University, Kakuma-machi, Kanazawa 920-1192, Japan

* Correspondence: maeda@se.kanazawa-u.ac.jp, yashima@chembio.nagoya-u.ac.jp

Table of Contents

1. Materials

Anhydrous THF and dichloromethane were obtained from Kanto Kagaku (Tokyo, Japan). Triethylamine (Et_3N) was dried over KOH pellets and distilled onto KOH under nitrogen. These solvents were stored under nitrogen. 1-Bromoethane and *N*,*N*-dimethyl-4-aminopyridine (DMAP) were purchased from Wako (Osaka, Japan). Pentanoic acid, *n*-butyl isocyanate, *n*-dodecyl isocyanate, tetradecanedioic acid, trimethylsilyldiazomethane, tridecanoic acid, 1-ethyl-3-(3-dimethylaminopropyl)carbodiimide hydrochloride (EDC-HCl), methylcyclohexane (MCH) were from Tokyo Kasei (TCI, Tokyo, Japan). Potassium carbonate (K_2CO_3) and (*R*)- and (*S*)-1-phenylethanol ((*R*)- and (*S*)-**A**) were obtained from Kanto Kagaku. Anhydrous acetonitrile, norbornadiene rhodium chloride dimer ($[Rh(nbd)Cl]_2$) and tetra-*n*-butylammonium fluoride (TBAF) (1.0 M in THF) were available from Aldrich (Milwaukee, WI, USA). The porous spherical silica gel with a mean particle size of 5 μm and a mean pore diameter of 30 nm (Daiso gel SP-300-5P) was kindly supplied from Daiso Chemicals (Osaka, Japan). ((2,2'-Bis(methoxymethoxy)-4'-hydroxy-4-biphenylyl)ethynyl)triisopropylsilane (**5**),[S1] (2,2'-bis(methoxymethoxy)-4'-dodecyloxycarbonyl-4-biphenylyl)acetylene (**2a**)[S2] and (2,2'-bis(methoxymethoxy)-4'-butoxycarbonyl-4-biphenylyl)acetylene (**2b**)[S3] were prepared according to the previously reported method.

2. Instruments

Melting points were measured on a Yanako melting point apparatus and were uncorrected. NMR spectra were taken on a JNM-ECA 500 (JEOL, Tokyo, Japan) (500 MHz for ^1H, 125 MHz for ^{13}C) spectrometer in $CDCl_3$ using tetramethylsilane (TMS) as the internal standard. IR spectra were recorded with a JASCO (Hachioji, Japan) Fourier Transform IR-460 spectrophotometer. Size exclusion chromatography (SEC) measurements were performed with a JASCO PU-2080 liquid chromatograph equipped with a photodiode array detector (JASCO MD-2018) at 40 °C. The temperature was controlled with a JASCO CO-1560 column oven. A Shodex (Tokyo, Japan) KF-805L (30 cm) column was used for SEC measurements and THF was used as the eluent at flow rate of 1.0 mL/min. The molecular weight calibration curves were obtained with polystyrene standards (Tosoh, Tokyo, Japan). Absorption and circular dichroism (CD) spectra were measured in a 1.0 mm quartz cell on a JASCO V-570 spectrophotometer and a JASCO J-725 spectropolarimeter, respectively. The temperature was controlled with a JASCO ETC-505T (absorption spectroscopy) and a JASCO PTC-348WI apparatus (CD spectroscopy). The chromatographic separations of enantiomers were performed using a JASCO PU-2080 liquid chromatograph equipped with a photodiode array detector (JASCO MD-2018) and a CD detector (JASCO CD-2095) at ca. 10 °C. Thermogravimetric (TG) analysis was conducted on a SEIKO

EXSTAR6000 TG/DTA 6200 (Seiko Instruments Inc., Chiba, Japan) under a heating rate of 30 °C/min. Vibrational circular dichroism (VCD) spectra were measured in a 0.15 mm BaF_2 cell with a JASCO JV-2001YS spectrometer equipped with a temperature controller (EYELA NCB-1200) (EYELA, Tokyo, Japan). The concentration was 40 mg/mL in MCH and toluene, and temperature was *ca*. –10 °C. All spectra were collected for *ca*. 4 h at a resolution of 4 cm^{-1}. Elemental analyses were performed by the Research Institute for Instrumental Analysis of Advanced Science Research Center, Kanazawa University, Kanazawa, Japan.

3. Synthesis

Biphenylylacetylene monomers (**1b**, **3a, 3b, 4a**, **4b**) were prepared according to Scheme S1.

Scheme S1. Synthesis of **1b**, **3a, 3b, 4a** and **4b**.

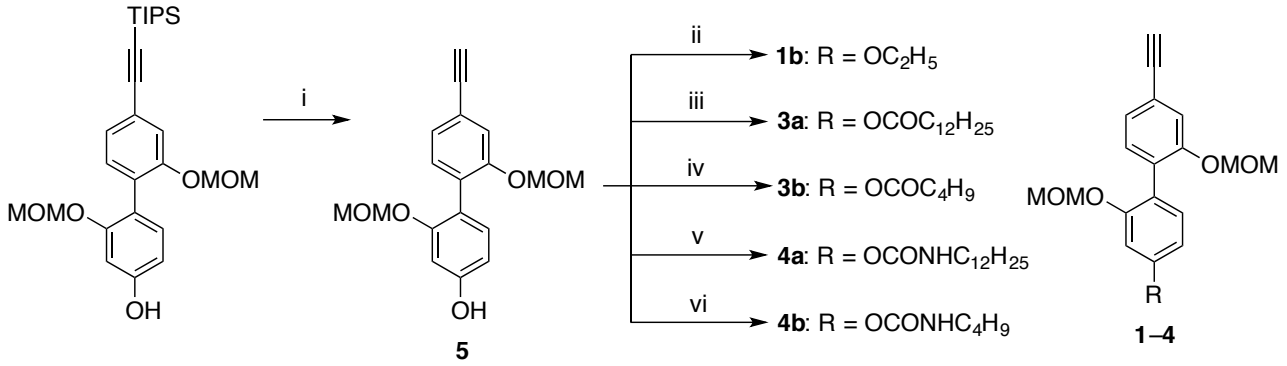

i) TBAF, THF, 0 °C, ii) 1-bromoethane, K_2CO_3, acetonitrile, reflux, iii) tridecanoic acid, DMAP, EDC-HCl, CH_2Cl_2, rt, iv) pentanoic acid, DMAP, EDC-HCl, CH_2Cl_2, rt, v) *n*-dodecyl isocyanate, Et_3N, CH_2Cl_2, rt, vi) *n*-butyl isocyanate, Et_3N, CH_2Cl_2, rt.

i) **(2,2'-Bis(methoxymethoxy)-4'-hydroxy-4-biphenylyl)acetylene (5)** To a solution of ((2,2'-bis(methoxymethoxy)-4'-hydroxy-4-biphenylyl)ethynyl)triisopropylsilane (3.03 g, 6.44 mmol) in THF (257 mL) was added TBAF (1.0 M in THF, 7.73 mL, 7.73 mmol). The mixture was stirred at 0 °C for 1 h and was diluted with ethyl acetate. The solution was washed with 1 N HCl aqueous solution and water, and then dried over Na_2SO_4. After filtration, the solvent was removed under reduced pressure and the crude product was then purified by silica gel chromatography using *n*-hexane—ethyl acetate (3/1, v/v) as the eluent to give the desired product as a pale yellow solid (1.98 g, 98% yield). Mp: 69.0–69.8 °C. IR (KBr, cm^{-1}): 3276 (≡CH), 2105 (C≡C). ^1H NMR (500 MHz, $CDCl_3$, rt): δ7.34 (s, 1H, Ar–H), 7.19–7.18 (m, 2H, Ar–H), 7.08 (d, J = 8.2 Hz, 1H, Ar–H), 6.76 (d, J = 2.3 Hz, 1H, Ar–H), 6.54 (dd, J = 5.9,

2.3 Hz, 1H, Ar–H), 5.05 (d, J = 6.4 Hz, 4H, 2OCH_2O), 4.78 (br-s, 1H, OH), 3.36 (d, J = 1.8 Hz, 6H, 2OCH_3), 3.08 (s, 1H, C≡C-H). ^{13}C NMR (125 MHz, CDCl_3, rt): δ 156.58, 156.10, 155.11, 132.23, 132.04, 130.26, 126.04, 122.29, 121.04, 119.40, 108.97, 103.52, 95.56, 95.44, 83.95, 77.23, 56.31, 56.27. Calcd for $C_{18}H_{18}O_5 \cdot (H_2O)_{0.3}$: C, 67.62; H, 5.86. Found: C, 67.60; H, 5.78.

ii) **(2,2'-Bis(methoxymethoxy)-4'-ethoxy-4-biphenylyl)acetylene** (**1b**) To a solution of **5** (200 mg, 0.64 mmol) in anhydrous acetonitrile (6.4 mL) was added K_2CO_3 (265 mg, 1.92 mmol) and 1-bromoethane (0.096 mL, 1.28 mmol). After reflux for 5 h, the mixture was diluted with ethyl acetate. The solution was washed with 1 N HCl aqueous solution and water, and then dried over Na_2SO_4. After filtration, the solvent was removed under reduced pressure and the crude product was then purified by silica gel chromatography using *n*-hexane—ethyl acetate (15/1, v/v) as the eluent to give the desired product as a white solid (210 mg, 96% yield). Mp: 54.6–55.3 °C. IR (KBr, cm^{-1}): 3246 (≡CH), 2100 (C≡C). ^{1}H NMR (500 MHz, CDCl_3, rt): δ 7.34 (s, 1H, Ar–H), 7.19 (s, 2H, Ar–H), 7.12 (d, J = 8.6 Hz, 1H, Ar–H), 6.80 (d, J = 2.0 Hz, 1H, Ar–H), 6.61–6.59 (dd, J = 5.7, 2.3 Hz, 1H, Ar–H), 5.05 (d, J = 6.3 Hz, 4H, 2OCH_2O), 4.06 (q, J = 6.9 Hz, 2H, COCH_2), 3.35 (d, J = 9.2 Hz, 6H, 2OCH_3), 3.08 (s, 1H, C≡C-H), 1.43 (t, J = 6.9 Hz, 3H, CH_2CH_3). ^{13}C NMR (125 MHz, CDCl_3, rt): δ 159.74, 155.69, 154.80, 131.73, 131.59, 130.10, 125.67, 121.85, 120.55, 119.08, 107.11, 102.79, 95.21 (2C), 83.65, 77.27, 63.54, 55.95, 55.93, 14.85. Calcd for $C_{20}H_{22}O_5 \cdot (H_2O)_{0.1}$: C, 69.79; H, 6.50. Found: C, 69.68; H, 6.56.

iii) **(2,2'-Bis(methoxymethoxy)-4'-dodecyloxyester-4-biphenylyl)acetylene (3a)** The compound **5** (200 mg, 0.64 mmol), tridecanoic acid (165 mg, 0.77 mmol), DMAP (93.8 mg, 0.77 mmol) were dissolved in anhydrous dichloromethane (7.0 mL) and the solution was cooled to 0 °C. To this solution was added EDC-HCl (160 mg, 0.83 mmol) and the mixture was stirred at rt for 3 h. After evaporating the solvent, the mixture was diluted with ethyl acetate, washed with water, and then dried over Na_2SO_4. The solvent was removed under reduced pressure and the crude product was purified by silica gel chromatography using *n*-hexane—ethyl acetate (10/3, v/v) as the eluent to give the desired product as a pale white solid (282 mg, 87% yield). Mp: 47.8–48.6 °C. IR (KBr, cm^{-1}): 3236 (≡CH), 2108 (C≡C), 1752 (C=O). ^{1}H NMR (500 MHz, CDCl_3, rt): δ 7.35 (s, 1H, Ar–H), 7.21-7.17 (m, 3H, Ar–H), 6.97 (d, J = 2.4 Hz, 1H, Ar–H), 6.81 (dd, J = 6.2, 2.0 Hz, 1H, Ar–H), 5.06 (s, 4H, 2OCH_2O), 3.35 (d, J = 1.7 Hz, 6H, 2OCH_3), 3.08 (s, 1H, C≡C-H), 2.56 (t, J = 7.6 Hz, 2H, COCH_2), 1.76 (quint, J = 7.6 Hz, 2H, CH_2CH_2), 1.43–1.27 (m, 18H, CH_2CH_2), 0.88 (t, J = 6.5 Hz, 3H, CH_2CH_3). ^{13}C NMR (125 MHz, CDCl_3, rt): δ 172.27, 155.41, 154.73, 151.08, 131.51, 131.46, 129.45, 125.67, 125.54, 122.37, 118.94, 114.77, 109.06, 95.18, 95.14, 83.52, 77.24, 55.99 (2C), 34.44, 31.93, 29.66, 29.64, 29.62, 29.48, 29.37, 29.29,

29.15, 24.91, 22.70, 14.14. Calcd for $C_{31}H_{42}O_6$: C, 72.91; H, 8.29. Found: C, 72.78; H, 8.37.

iv) **(2,2'-Bis(methoxymethoxy)-4'-pentanoyloxyester-4-biphenylyl)acetylene (3b)** The compound **5** (200 mg, 0.64 mmol), pentanoic acid (78.3 mg, 0.77 mmol) and DMAP (93.8 mg, 0.77 mmol) were dissolved in anhydrous dichloromethane (20 mL) and the solution was cooled to 0 °C. To this solution was added EDC-HCl (148 mg, 0.77 mmol) and the mixture was stirred at rt for 3 h. After evaporating the solvent, the mixture was diluted with ethyl acetate, and the solution was washed with water, and then dried over Na_2SO_4. The solvent was removed under reduced pressure and the crude product was purified by silica gel chromatography using *n*-hexane—ethyl acetate (7/2, v/v) as the eluent to give the desired product as a pale white solid (246 mg, 97% yield). Mp: 45.3–46.3 °C. IR (KBr, cm^{-1}): 3259 (≡CH), 2103 (C≡C), 1761 (C=O). ^1H NMR (500 MHz, $CDCl_3$, rt): δ 7.35 (s, 1H, Ar–H), 7.21–7.16 (m, 3H, Ar–H), 6.97 (d, J = 2.3 Hz, 1H, Ar–H), 6.81 (dd, J = 6.0, 2.3 Hz, 1H, Ar–H), 5.06 (s, 4H, $2OCH_2O$), 3.35 (d, J = 1.4 Hz, 6H, $2OCH_3$), 3.09 (s, 1H, C≡C-H), 2.56 (t, J = 7.8 Hz, 2H, $COCH_2$), 1.75 (quint, J = 7.3 Hz, 2H, CH_2CH_2), 1.46 (sex, J = 7.8 Hz, 2H, CH_2CH_2), 0.98 (t, J = 7.3 Hz, 3H, CH_2CH_3). ^{13}C NMR (125 MHz, $CDCl_3$, rt): δ 172.24, 155.41, 154.72, 151.07, 131.50, 131.46, 129.45, 125.66, 125.55, 122.36, 118.94, 114.79, 109.04, 95.18, 95.14, 83.52, 77.21, 55.99 (2C), 34.14, 26.96, 22.27, 13.75. Calcd for $C_{23}H_{26}O_6$: C, 69.33; H, 6.58. Found: C, 69.33; H, 6.65.

v) **(2,2'-Bis(methoxymethoxy)-4'-dodecylcarbamoyloxy-4-biphenylyl)acetylene** (**4a**) To a solution of **5** (100 mg, 0.32 mmol) in anhydrous diethyl ether (3.0 mL) was added Et_3N (4 drops) and *n*-dodecyl isocyanate (0.15 mL, 0.64 mmol). After stirring at rt for 3 h, the mixture was diluted with ethyl acetate, and the solution was washed with 1 N HCl aqueous solution and water, and then dried over Na_2SO_4. After evaporating the solvent, the crude product was purified by silica gel chromatography using *n*-hexane—ethyl acetate (5/1, v/v) as the eluent to give the desired product as a white solid (160 mg, 96% yield). Mp: 65.3–66.1 °C. IR (KBr, cm^{-1}): 3363 (N-H), 3286 (≡CH), 2106 (C≡C), 1711 (C=O). ^1H NMR ($CDCl_3$, 500 MHz, rt): δ 7.35 (s, 1H, Ar–H), 7.21–7.16 (m, 3H, Ar–H), 7.02 (d, J = 2.3 Hz, 1H, Ar–H), 6.86 (dd, J = 6.0, 2.3 Hz, 1H, Ar–H), 5.06 (s, 4H, $2OCH_2O$), 5.00 (t, J = 5.5 Hz, 1H, CONH), 3.35 (d, J = 2.3 Hz, 6H, $2OCH_3$), 3.27 (q, J = 6.4 Hz, 2H, $NHCH_2$), 3.08 (s, 1H, C≡C-H), 1.58 (quint, J = 6.9 Hz, 2H, CH_2CH_2), 1.34–1.27 (m, 18H, CH_2CH_2), 0.88 (t, J = 6.9 Hz, 3H, CH_2CH_3). ^{13}C NMR (125 MHz, $CDCl_3$, rt): δ 155.26, 154.73, 154.39, 151.40, 131.53, 131.33, 129.57, 125.63, 125.04, 122.25, 118.90, 114.82, 109.12, 95.11 (2C), 83.55, 77.13, 55.98 (2C), 41.31, 31.91, 29.83, 29.63, 29.66, 29.59, 29.55, 29.34, 29.29, 26.77, 22.69, 14.13. Calcd for $C_{31}H_{43}NO_6$: C, 70.83; H, 8.25; N, 2.66. Found: C, 70.80; H,

8.33; N, 2.71.

vi) **(2,2'-Bis(methoxymethoxy)-4'-butylcarbamoyloxy-4-biphenylyl)acetylene** (**4b**) To a solution of **5** (1.87 g, 5.95 mmol) in anhydrous diethyl ether (60 mL) was added Et_3N (1.2 mL) and *n*-butyl isocyanate (0.80 mL, 7.13 mmol). After stirring at rt for 3 h, the mixture was diluted with ethyl acetate, and the solution was washed with 1 N HCl aqueous solution and water, and then dried over Na_2SO_4. After evaporating the solvent, the crude product was purified by silica gel chromatography using *n*-hexane—ethyl acetate (5/1, v/v) as the eluent to give the desired product as a white solid (2.08 g, 85% yield). Mp: 85.3–86.1 °C. IR (KBr, cm^{-1}): 3363 (N-H), 3241 (≡CH), 2106 (C≡C), 1712 (C=O). ^{1}H NMR ($CDCl_3$, 500 MHz, rt): δ 7.35 (s, 1H, Ar–H), 7.21–7.16 (m, 3H, Ar–H), 7.02 (d, J = 1.8 Hz, 1H, Ar–H), 6.86 (dd, J = 8.5, 2.1 Hz, 1H, Ar–H), 5.06 (s, 4H, $2OCH_2O$), 5.00 (t, J = 5.4 Hz, 1H, CONH), 3.35 (d, J = 2.8 Hz, 6H, $2OCH_3$), 3.29 (q, J = 7.2 Hz, 2H, $NHCH_2$), 3.08 (s, 1H, C≡C-H), 1.57 (quint, J = 7.2 Hz, 2H, CH_2CH_2), 1.41 (sex, J = 7.6 Hz, 2H, CH_2CH_2), 0.97 (t, J = 7.6 Hz, 3H, CH_2CH_3). ^{13}C NMR (125 MHz, $CDCl_3$, rt): δ 155.22, 154.70, 154.40, 151.37, 131.51, 131.30, 129.53, 125.60, 125.02, 122.22, 118.85, 114.80, 109.08, 95.09, 95.08, 83.52, 77.13, 55.95, 53.42, 40.95, 31.87, 19.89, 13.72. Calcd for $C_{23}H_{27}NO_6$: C, 66.81; H, 6.58; N, 3.39. Found: C, 66.59; H, 6.63; N, 3.34.

4. Polymerization

Cis-transoidal stereoregular poly-**2a**[S2] and poly-**2b**[S3] were prepared according to the previously reported method.[S4] The number-average molecular weight (M_n) and its distribution (M_w/M_n) were estimated to be 8.5 × 10^5 and 1.9 (poly-**2a**) and 9.4 × 10^5 and 1.7 (poly-**2b**), respectively, by size exclusion chromatography (SEC) with polystyrene standards in THF. Homopolymerization of **1b**, **3** and **4** and copolymerization of **5** with **2b, 3b** and **4b** were carried out in a dry glass ampule under a dry nitrogen atmosphere using $[Rh(nbd)Cl]_2$ as a catalyst in the same way as reported previously (Scheme S2).[S1-4] The results of the homopolymerization and copolymerization are summarized in Table 1 and Table 3, respectively.

Scheme S2. Synthesis of poly**1b**, poly-**3**, poly-**4**, poly(**2b**-*co*-**5**), poly(**3b**-*co*-**5**) and poly(**4b**-*co*-**5**)

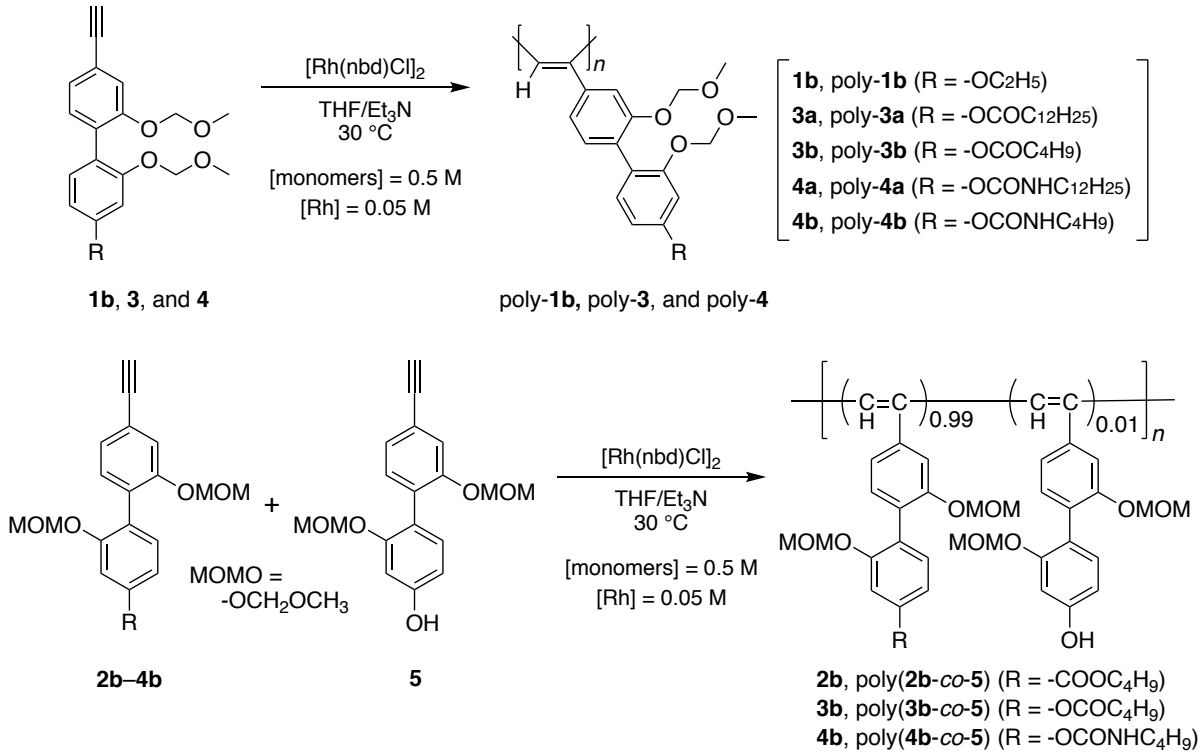

Spectroscopic data of poly-**1b**. ^{1}H NMR (500 MHz, $CDCl_3$, 55 °C): δ 6.95–6.30 (br, 6H, Ar–H), 6.10–5.90 (br, 1H, C=CH), 4.85–4.60 (br, 4H, $2OCH_2O$), 4.00–3.80 (br, 2H, OCH_2), 3.20–2.90 (br, 6H, $2OCH_3$), 1.40–1.20 (br, 3H, CH_2CH_3). Calcd for $C_{20}H_{22}O_5\cdot(H_2O)_{0.1}$: C, 69.79; H, 6.50. Found: C, 69.75; H, 6.52.

Spectroscopic data of poly-**3a**. IR (KBr, cm^{-1}): 1760 (C=O). ^{1}H NMR (500 MHz, $CDCl_3$, 55 °C): δ 6.95–6.40 (br, 6H, Ar–H), 6.20–5.95 (br, 1H, C=CH), 4.88–4.60 (br, 4H, $2OCH_2O$), 3.15–2.90 (br, 6H, $2OCH_3$), 2.55–2.35 (br, 2H, OCH_2), 1.80–1.64 (br, 2H, CH_2CH_2), 1.45–1.20 (br, 18H, CH_2CH_2), 0.93–0.85 (br, 3H, CH_2CH_3). Calcd for $C_{31}H_{42}O_6\cdot(H_2O)_{0.1}$: C, 72.66; H, 8.30. Found: C, 72.53; H, 8.28.

Spectroscopic data of poly-**3b**. IR (KBr, cm^{-1}): 1758 (C=O). ^{1}H NMR (500 MHz, $CDCl_3$, 55 °C): δ 6.96–6.36 (br, 6H, Ar–H), 6.05–5.90 (br, 1H, C=CH), 4.91–4.55 (br, 4H, $2OCH_2O$), 3.20–2.89 (br, 6H, $2OCH_3$), 2.55–2.40 (br, 2H, OCH_2), 1.75–1.64 (br, 2H, CH_2CH_2), 1.47–1.36 (br, 2H, CH_2CH_2), 1.00–0.90 (br, 3H, CH_2CH_3). Calcd for $C_{23}H_{26}O_6$: C, 69.33; H, 6.58. Found: C, 69.06; H, 6.55.

Spectroscopic data of poly-**4a**. IR (KBr, cm^{-1}): 3406 (N-H), 1734 (C=O). ^{1}H NMR (500 MHz, $CDCl_3$, 55 °C): δ 7.0–6.30 (br, 6H, Ar–H), 6.05–5.85 (br, 1H, C=CH), 5.30–5.10 (br, 1H, NH), 4.90–4.45 (br, 4H, $2OCH_2O$), 3.30–2.85 (br, 2H, $NHCH_2$), (br, 6H, $2OCH_3$), 1.63–1.45 (br, 2H, CH_2CH_2), 1.40–1.10

(br, 18H, CH_2CH_2), 0.93–0.80 (br, 3H, CH_2CH_3). Calcd for $C_{31}H_{43}NO_6 \cdot (H_2O)_{0.1}$: C, 70.59; H, 8.26; N, 2.66. Found: C, 70.46; H, 8.33; N, 2.63.

Spectroscopic data of poly-**4b**. IR (KBr, cm^{-1}): 3347 (N-H), 1743 (C=O). ^1H NMR (500 MHz, $CDCl_3$, 55 °C): δ 7.05–6.30 (br, 6H, Ar–H), 6.10–5.85 (br, 1H, C=CH), 5.35–5.05 (br, 1H, NH), 5.00–4.40 (br, 4H, $2OCH_2O$), 3.40–2.80 (br, 2H, $NHCH_2$), (br, 6H, $2OCH_3$), 1.60–1.30 (br, 4H, CH_2CH_2), 1.0–0.90 (br, 3H, CH_2CH_3). Calcd for $C_{23}H_{27}NO_6 \cdot (H_2O)_{0.1}$: C, 66.52; H, 6.60; N, 3.37. Found: C, 66.31; H, 6.71; N, 3.35.

Spectroscopic data of poly(**2b**-*co*-**5**). IR (KBr, cm^{-1}): 1717 (C=O). ^1H NMR (500 MHz, $CDCl_3$, 55 °C): δ 7.80–6.40 (br, 6H, Ar–H), 6.10–5.95 (br, 1H, C=CH), 4.95–4.60 (br, 4H, $2OCH_2O$), 4.35–4.15 (br, 2H, OCH_2), 3.15–2.90 (br, 6H, $2OCH_3$), 1.75–1.64 (br, 2H, CH_2CH_2), 1.48–1.36 (br, 2H, CH_2CH_2), 0.98–0.89 (br, 3H, CH_2CH_3). Calcd for $C_{23}H_{26}O_6 \cdot (H_2O)_{0.2}$: C, 68.70; H, 6.60. Found: C, 68.76; H, 6.59

Spectroscopic data of poly(**3b**-*co*-**5**). IR (KBr, cm^{-1}): 1758 (C=O). ^1H NMR (500 MHz, $CDCl_3$, 55 °C): δ 6.96–6.30 (br, 6H, Ar–H), 6.05–5.90 (br, 1H, C=CH), 4.90–4.55 (br, 4H, $2OCH_2O$), 3.20–2.86 (br, 6H, $2OCH_3$), 2.55–2.35 (br, 2H, OCH_2), 1.75–1.62 (br, 2H, CH_2CH_2), 1.48–1.37 (br, 2H, CH_2CH_2), 1.00–0.90 (br, 3H, CH_2CH_3). Calcd for $C_{23}H_{26}O_6 \cdot (H_2O)_{0.1}$: C, 69.01; H, 6.59. Found: C, 68.94; H, 6.61.

Spectroscopic data of poly(**4b**-*co*-**5**). IR (KBr, cm^{-1}): 3347 (N-H), 1743 (C=O). ^1H NMR (500 MHz, $CDCl_3$, 55 °C): δ 7.10–6.30 (br, 6H, Ar–H), 6.10–5.90 (br, 1H, C=CH), 5.35–5.10 (br, 1H, NH), 5.00–4.50 (br, 4H, $2OCH_2O$), 3.40–2.80 (br, 2H, $NHCH_2$), (br, 6H, $2OCH_3$), 1.60–1.30 (br, 4H, CH_2CH_2), 1.0–0.90 (br, 3H, CH_2CH_3). Calcd for $C_{23}H_{27}NO_6 \cdot (H_2O)_{0.1}$: C, 66.54; H, 6.59; N, 3.34. Found: C, 66.48; H, 6.59; N, 3.34.

5. Preparation of coated-type chiral packing materials using optically active poly-1b–poly-4b with helicity memory

As-prepared, optically inactive poly-**1b**–poly-**3b** and poly-**4b** (60 mg) dissolved in a mixture of toluene/(*R*)-**A** (80/20, v/v, 2 mL) and THF/(*R*)-**A** (60/40, v/v; 2 mL), respectively, were allowed to stand at 25 °C for 48 h to completely induce an almost one-handed helical conformation. The resulting polymer solutions were then coated on macroporous silica gel (390 mg) according to the previously reported method,[S5] and the solvents were evaporated under reduced pressure. The contents of the polymers on silica gel were estimated to be ca. 13 wt% by thermogravimetric (TG) analysis.

6. Immobilization of poly(2b-*co*-5), poly(3b-*co*-5) and poly(4b-*co*-5) onto silica gel

A typical procedure for immobilization of poly(**2b**-*co*-**5**) onto silica gel is described as follows. As-prepared poly(**2b**-*co*-**5**) (90 mg) dissolved in THF (2.5 mL) was coated on macroporous silica gel (585 mg) in a similar way to that described in Section 5. The poly(**2b**-*co*-**5**)-coated silica gel (630 mg) was then dispersed in DMSO (12.6 mL). To this was added tetradecanedioic acid (**6**) (282 mg, 1.09 mmol) and DMAP (267 mg, 2.20 mmol) under a nitrogen atmosphere. After cooling to 0 °C, EDC-HCl (422 mg, 2.20 mmol) was then added to the suspended mixture, which was shaken at rt for 5 h. After filtration, the resulting silica gel was washed with THF (300 mL), dichloromethane (300 mL) and ethanol (300 mL) to remove non-immobilized poly(**2b**-*co*-**5**) and unreacted/partially reacted **6**, and dried in vacuo at rt overnight. The silica gel was then treated with trimethylsilyldiazomethane (2.0 M in diethyl ether, 0.37 mL, 0. 74 mmol) in methanol (20 mL) at rt for 5 h under a nitrogen atmosphere to convert the **6**-derived carboxy groups remaining in the cross-linked polymer (Si-poly(**2b**-*co*-**5**)) immobilized onto silica gel into methyl esters. The Si-poly(**2b**-*co*-**5**)-based immobilized-type packing material thus obtained was collected by filtration, washed with THF (300 mL), dichloromethane (300 mL), ethanol (300 mL), toluene/*rac*-**A** (50/50, v/v, 20 mL) and *n*-hexane (300 mL), and then dried in vacuo at rt overnight. In the same way, the Si-poly(**3b**-*co*-**5**)- and Si-poly(**4b**-*co*-**5**)-based immobilized-type packing materials were prepared. The contents of the cross-linked polymers (Si-poly(**2b**-*co*-**5**), Si-poly(**3b**-*co*-**5**) and Si-poly(**4b**-*co*-**5**)) immobilized onto silica gel were estimated to be 9.9, 10 and 9.2 wt%, respectively, by TG analysis.

Table S1. Immobilization results of the poly(**2**-*co*-**5**), poly(**3**-*co*-**5**) and poly(**4**-*co*-**5**)

run	sample code	copolymer	coating amount[a] (wt%)	immobilized amount[a] (wt%)	immobilization efficiency (%)
1	Si-poly(**2b**-*co*-**5**)	poly(**2b**-*co*-**5**)	13	9.9	76
2	Si-poly(**3b**-*co*-**5**)	poly(**3b**-*co*-**5**)	13	10	77
3	Si-poly(**4b**-*co*-**5**)	poly(**4b**-*co*-**5**)	13	9.2	71

[a] Determined by TG analysis.

7. Preparation of HPLC columns

After the packing materials were fractionated with sieves, the fractionated packing materials were then packed into a stainless-steel column (25 cm × 0.20 cm (i.d.)) by a conventional high-pressure slurry packing technique using an ECONO-PACKER MODEL CPP-085 (Chemco, St Louis, MO).[S6] The numbers of theoretical plates of all the coated- and immobilized-type columns were estimated to be ca. 3000 for benzene using an *n*-hexane–2-propanol (97/3, v/v) mixture as the eluent at a flow rate of 0.2

mL/min at ca. 10 °C. The hold-up time (t_0) was estimated using 1,3,5-tri-*tert*-butylbenzene as the non-retained compound.[S7]

8. Reversible control of the macromolecular helicity of the immobilized polymers in the column

A typical procedure for the reversible control of the macromolecular helicity of the Si-poly(**3b**-*co*-**5**) immobilized onto silica gel in the column is described as follows.

8-1. Helicity induction and its static memory of the immobilized polymers in the column

The Si-poly(**3b**-*co*-**5**)-based immobilized-type column was filled with (*R*)-**A** in toluene ((*R*)-**A**/toluene = 50/50, v/v) and allowed to stand at 25 °C for 24 h to induce a preferred-handed helicity (*P*-helix) in the immobilized Si-poly(**3b**-*co*-**5**) backbone in the column. The toluene solution of (*R*)-**A** in the column was then completely replaced with a mixture of *n*-hexane/2-propanol (97/3, v/v) by flowing an excess amount of hexane/2-propanol (97/3, v/v) at ca. 10 °C for 120 min at a flow rate of 0.05 mL/min, which resulted in a CSP consisting of *P*-Si-poly(**3b**-*co*-**5**) with right-handed helicity memory. The chiral recognition ability of *P*-Si-poly(**3b**-*co*-**5**) was then investigated by HPLC under normal-phase conditions (eluent, hexane/2-propanol (97/3, v/v); flow rate, 0.2 mL/min; temperature, ca. 10 °C).

8-2. Reversible switching of the helical sense of the immobilized polymers in the column

The *P*-Si-poly(**3b**-*co*-**5**)-based immobilized-type column was filled with dichloromethane and allowed to stand at 25 °C for 2 h to erase the helicity memory. After removing the dichloromethane in the column in vacuo at rt, the column was filled with (*S*)-**A** in toluene ((*S*)-**A**/toluene = 50/50, v/v) and allowed to stand at 25 °C for 24 h to induce the left-handed helicity in the immobilized Si-poly(**3b**-*co*-**5**) backbone in the column, whose helical handedness was opposite to that of *P*-Si-poly(**3b**-*co*-**5**). By replacing the toluene solution of (*S*)-**A** in the column with a mixture of *n*-hexane/2-propanol (97/3, v/v) in the same way as described above, a CSP consisting of *M*-Si-poly(**3b**-*co*-**5**) with left-handed helicity memory was obtained. The column packed with *M*-Si-poly(**3b**-*co*-**5**) was further treated with dichloromethane followed by (*R*)-**A** in toluene ((*R*)-**A**/toluene = 50/50, v/v) and then replacement with a mixture of *n*-hexane/2-propanol (97/3, v/v) in the same way, to give a CSP composed of *P*'-Si-poly(**3b**-*co*-**5**) with a right-handed helicity memory.

In the same way, the reversible switching of the macromolecular helicity memory of the Si-poly(**2b**-*co*-**5**)- and Si-poly(**4b**-*co*-**5**)-based immobilized-type columns was performed.

9. Supporting data

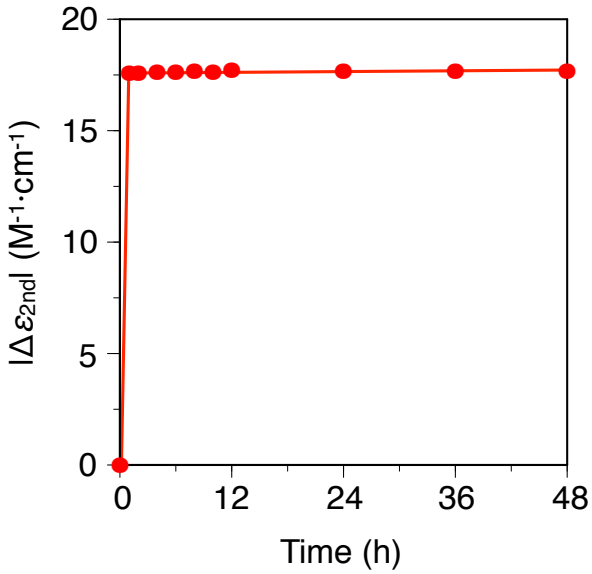

Fig. S1. Time-dependent CD intensity ($|\Delta\varepsilon_{2nd}|$) change of poly-**1a** in toluene/(*R*)-**A** (80/20, v/v) at 25 °C. [Poly-**1a**] = 1.0 mM.

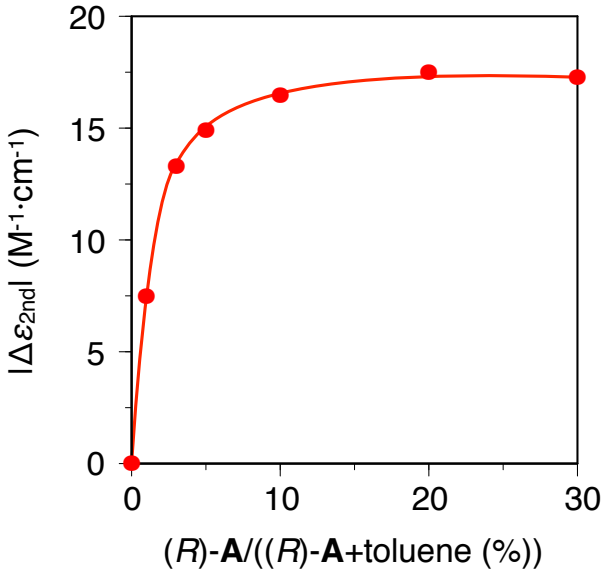

Fig. S2. CD titration curve ($|\Delta\varepsilon_{2nd}|$) of poly-**1a** with (*R*)-**A** in toluene at 25 °C after standing at 25 °C for 48 h. [Poly-**1a**] = 1.0 mM.

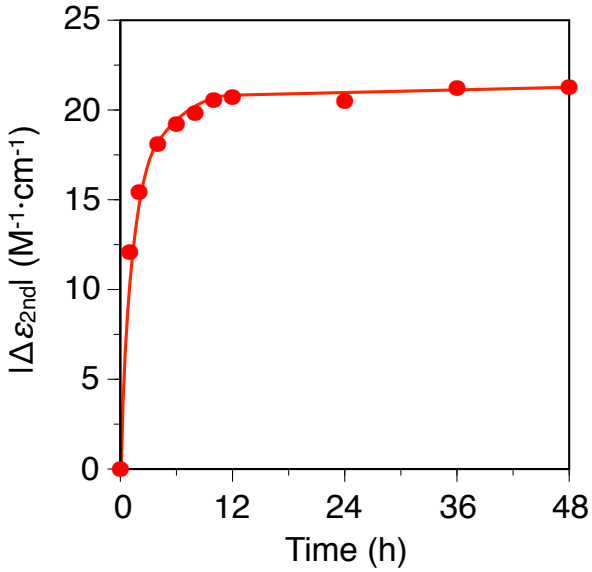

Fig. S3. Time-dependent CD intensity ($|\Delta\varepsilon_{2nd}|$) change of poly-**2a** in toluene/(*R*)-**A** (80/20, v/v) at 25 °C. [Poly-**2a**] = 1.0 mM.

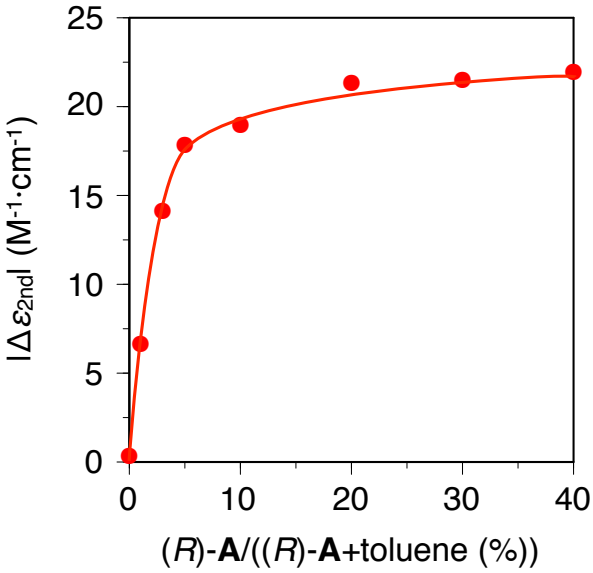

Fig. S4. CD titration curve ($|\Delta\varepsilon_{2nd}|$) of poly-**2a** with (*R*)-**A** in toluene at 25 °C after standing at 25 °C for 48 h. [Poly-**2a**] = 1.0 mM.

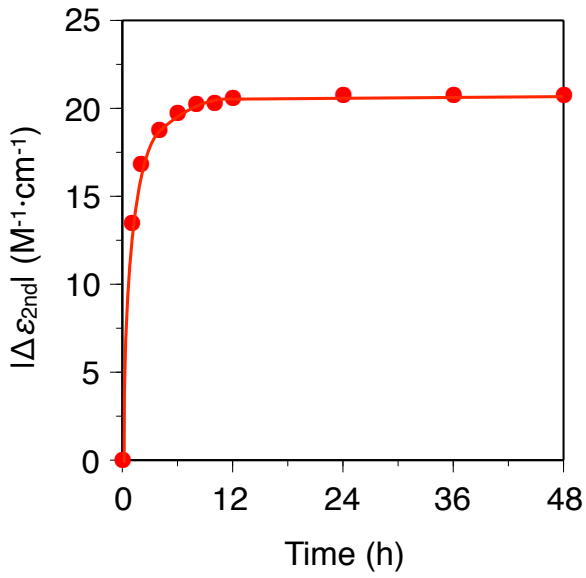

Fig. S5. Time-dependent CD intensity ($|\Delta\varepsilon_{2nd}|$) change of poly-**3a** in toluene/(*R*)-**A** (80/20, v/v) at 25 °C. [Poly-**3a**] = 1.0 mM.

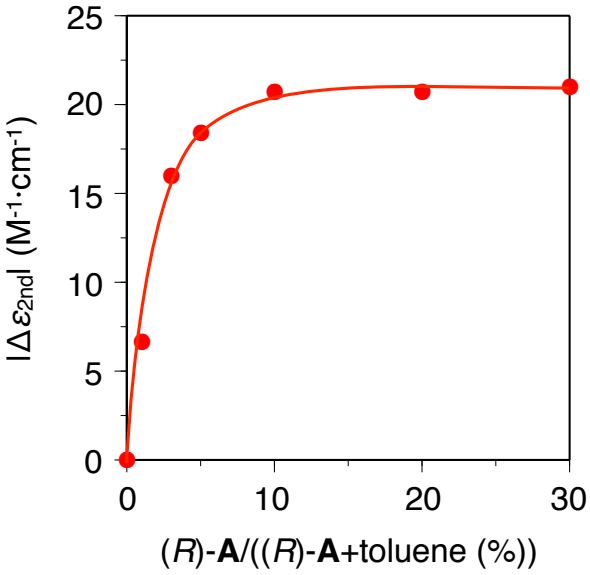

Fig. S6. CD titration curve ($|\Delta\varepsilon_{2nd}|$) of poly-**3a** with (*R*)-**A** in toluene at 25 °C after standing at 25 °C for 48 h. [Poly-**3a**] = 1.0 mM.

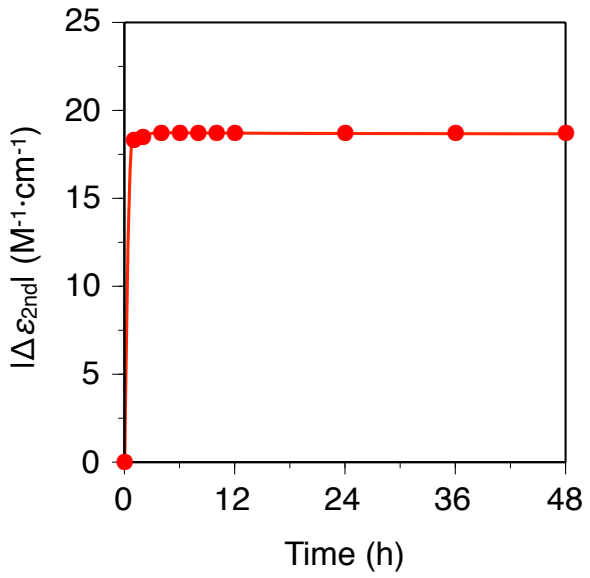

Fig. S7. Time-dependent CD intensity ($|\Delta\varepsilon_{2nd}|$) change of poly-**4a** in toluene/(*R*)-**A** (80/20, v/v) at 25 °C. [Poly-**4a**] = 1.0 mM.

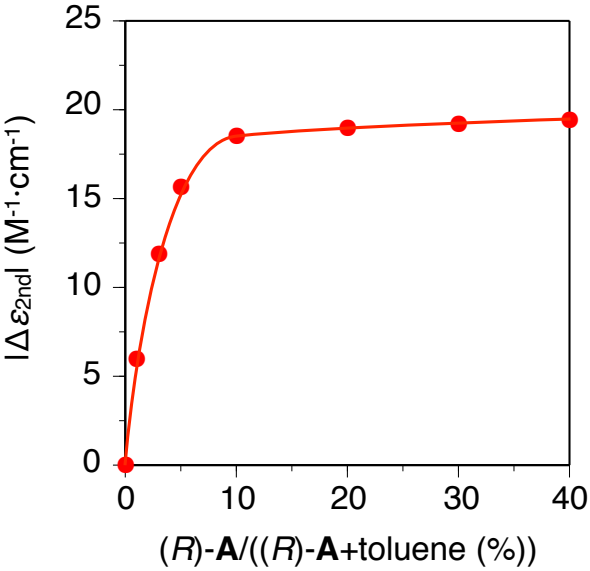

Fig. S8. CD titration curve ($|\Delta\varepsilon_{2nd}|$) of poly-**4a** with (*R*)-**A** in toluene at 25 °C after standing at 25 °C for 48 h. [Poly-**4a**] = 1.0 mM.

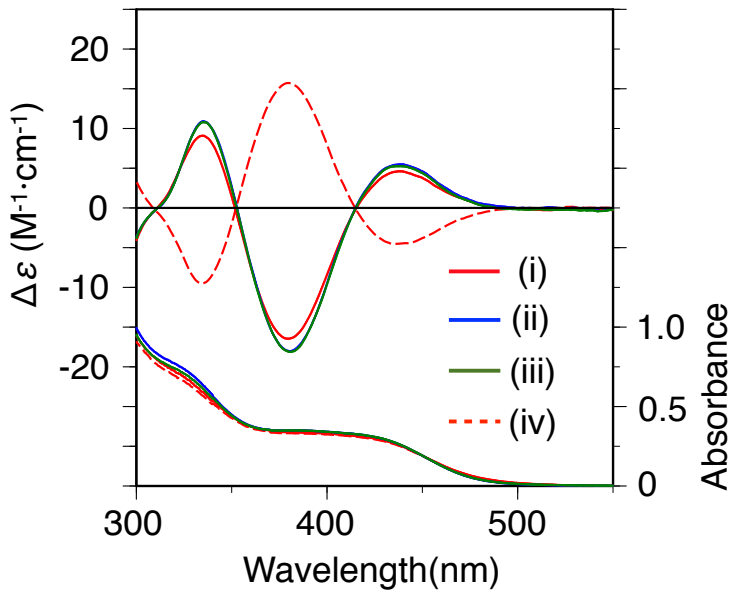

Fig. S9. CD and absorption spectra of poly-**1b** in toluene with (*R*)-**A** (toluene/(*R*)-**A** = 80/20, v/v) at 25 °C (i) and –10 °C (ii) after standing at 25 °C for 48 h, and the isolated poly-**1b** from ii (iii) measured in toluene at –10 °C. CD and absorption spectra of poly-**1b** in toluene with (*S*)-**A** (toluene/(*S*)-**A** = 80/20, v/v) at 25 °C (iv) after standing at 25 °C for 48 h are also shown. [Poly-**1b**] = 1.0 mM.

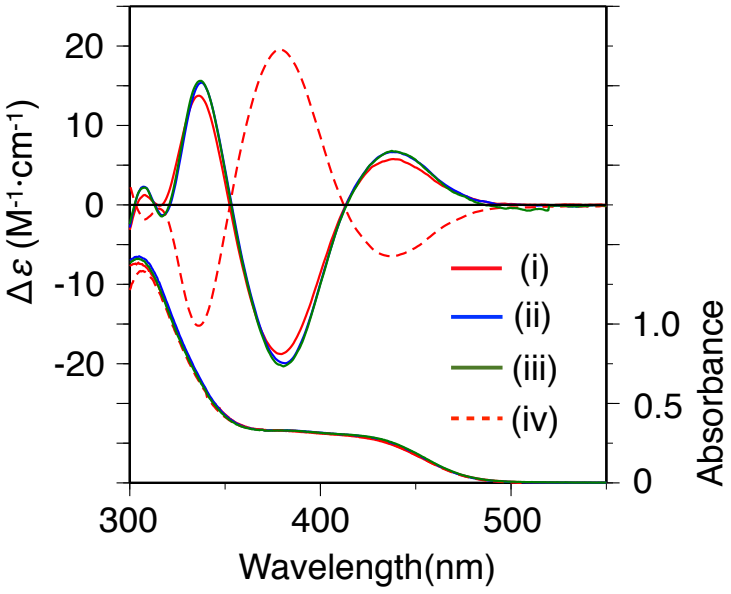

Fig. S10. CD and absorption spectra of poly-**2b** in toluene with (*R*)-**A** (toluene/(*R*)-**A** = 80/20, v/v) at 25 °C (i) and –10 °C (ii) after standing at 25 °C for 48 h, and the isolated poly-**2b** from ii (iii) measured in toluene at –10 °C. CD and absorption spectra of poly-**2b** in toluene with (*S*)-**A** (toluene/(*S*)-**A** = 80/20, v/v) at 25 °C (iv) after standing at 25 °C for 48 h are also shown. [Poly-**2b**] = 1.0 mM.

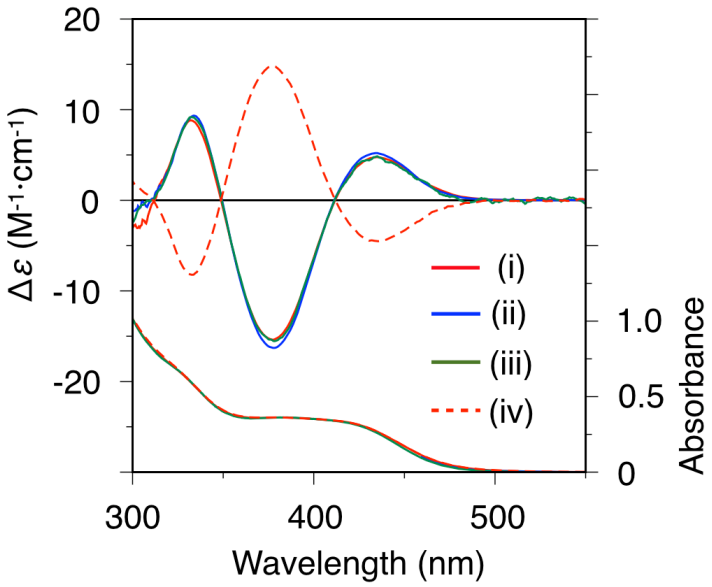

Fig. S11. CD and absorption spectra of poly-**3b** in toluene with (*R*)-**A** (toluene/(*R*)-**A** = 80/20, v/v) at 25 °C (i) and –10 °C (ii) after standing at 25 °C for 48 h, and the isolated poly-**3b** from ii (iii) measured in toluene at –10 °C. CD and absorption spectra of poly-**3b** in toluene with (*S*)-**A** (toluene/(*S*)-**A** = 80/20, v/v) at 25 °C (iv) after standing at 25 °C for 48 h are also shown. [Poly-**3b**] = 1.0 mM.

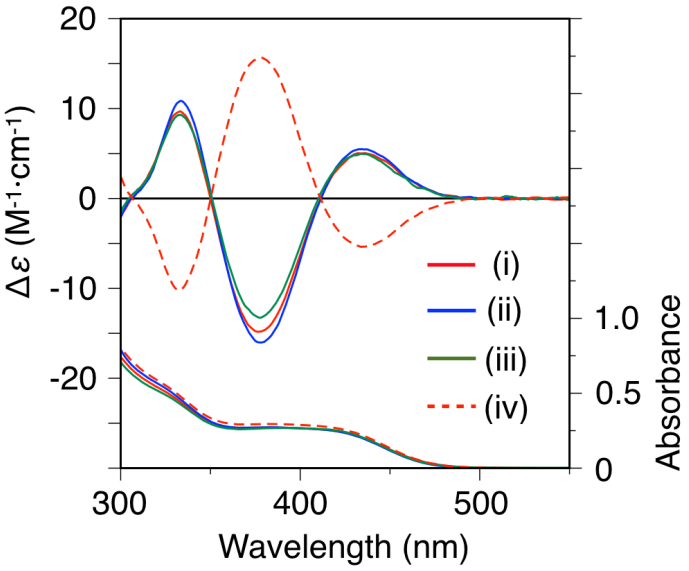

Fig. S12. CD and absorption spectra of poly-**4b** in THF with (*R*)-**A** (THF/(*R*)-**A** = 60/40, v/v) at 25 °C (i) and –10 °C (ii) after standing at 25 °C for 48 h, and the isolated poly-**4b** from ii (iii) measured in THF at –10 °C. CD and absorption spectra of poly-**4b** in THF with (*S*)-**A** (THF/(*S*)-**A** = 60/40, v/v) at 25 °C (iv) after standing at 25 °C for 48 h are also shown. [Poly-**4b**] = 1.0 mM.

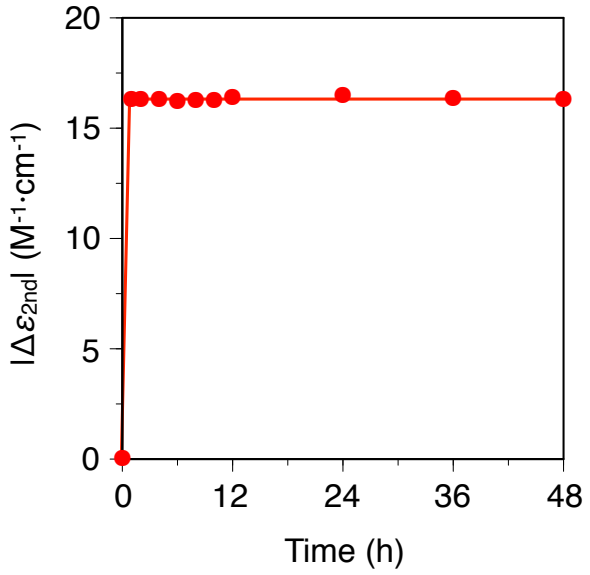

Fig. S13. Time-dependent CD intensity ($|\Delta\varepsilon_{2nd}|$) change of poly-**1b** in toluene/(*R*)-**A** (80/20, v/v) at 25 °C. [Poly-**1b**] = 1.0 mM.

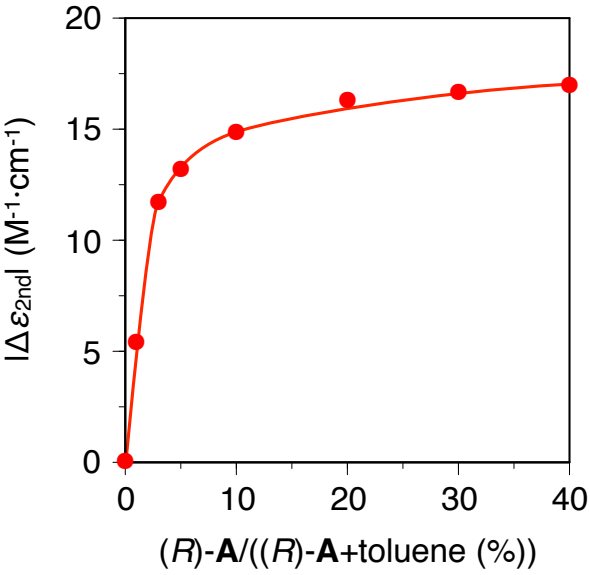

Fig. S14. CD titration curve ($|\Delta\varepsilon_{2nd}|$) of poly-**1b** with (*R*)-**A** in toluene at 25 °C after standing at 25 °C for 48 h. [Poly-**1b**] = 1.0 mM.

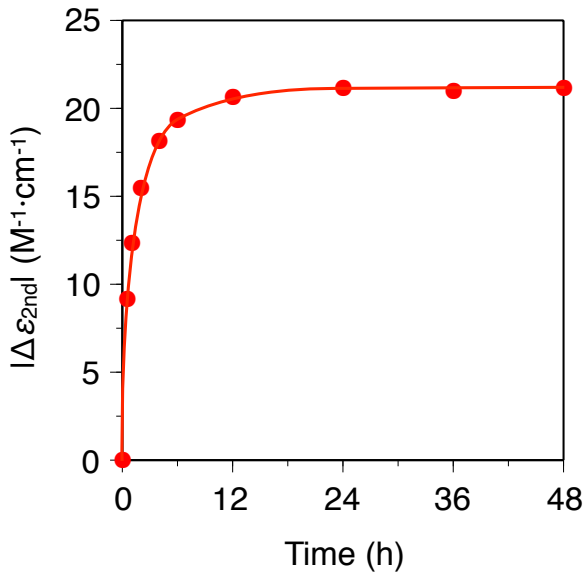

Fig. S15. Time-dependent CD intensity ($|\Delta\varepsilon_{2nd}|$) change of poly-**2b** in toluene/(*R*)-**A** (80/20, v/v) at 25 °C. [Poly-**2b**] = 1.0 mM.[S3]

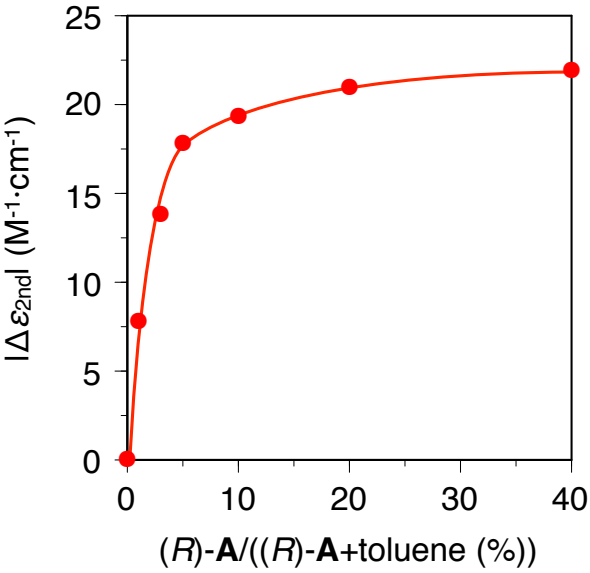

Fig. S16. CD titration curve ($|\Delta\varepsilon_{2nd}|$) of poly-**2b** with (*R*)-**A** in toluene at 25 °C after standing at 25 °C for 48 h. [Poly-**2b**] = 1.0 mM.[S3]

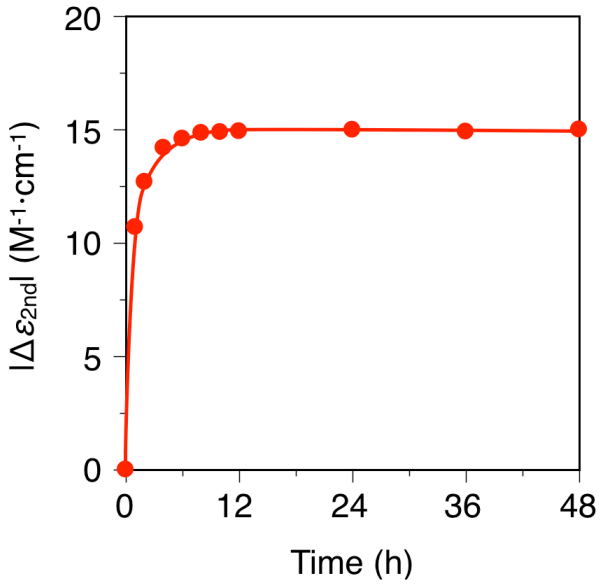

Fig. S17. Time-dependent CD intensity ($|\Delta\varepsilon_{2nd}|$) change of poly-**3b** in toluene/(*R*)-**A** (80/20, v/v) at 25 °C. [Poly-**3b**] = 1.0 mM.

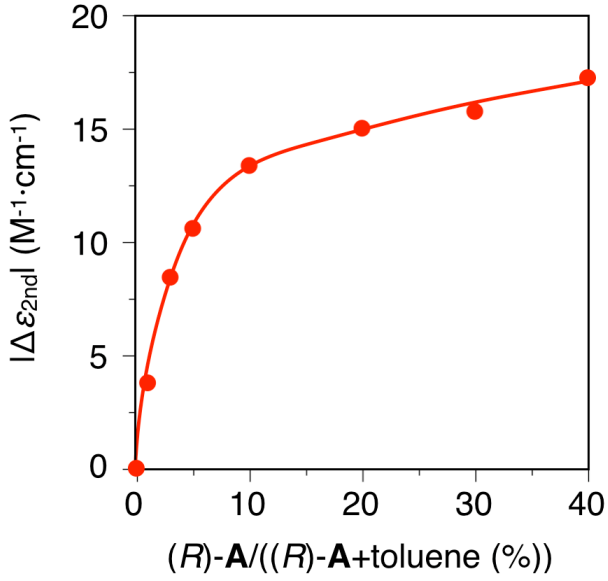

Fig. S18. CD titration curve ($|\Delta\varepsilon_{2nd}|$) of poly-**3b** with (*R*)-**A** in toluene at 25 °C after standing at 25 °C for 48 h. [Poly-**3b**] = 1.0 mM.

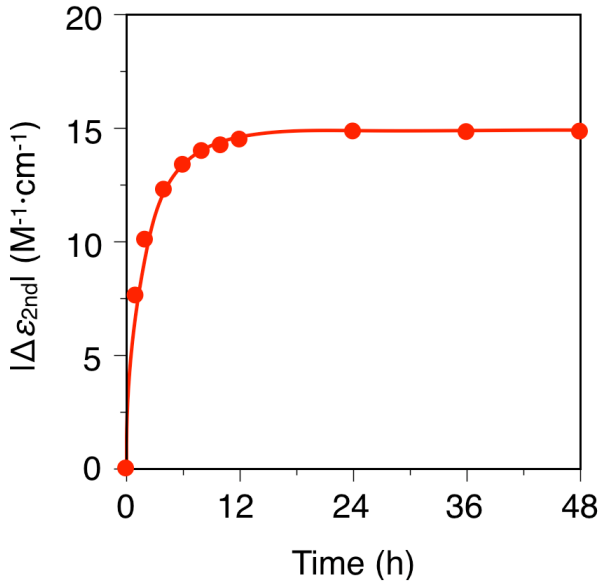

Fig. S19. Time-dependent CD intensity ($|\Delta\varepsilon_{2nd}|$) change of poly-**4b** in THF/(*R*)-**A** (60/40, v/v) at 25 °C. [Poly-**4b**] = 1.0 mM.

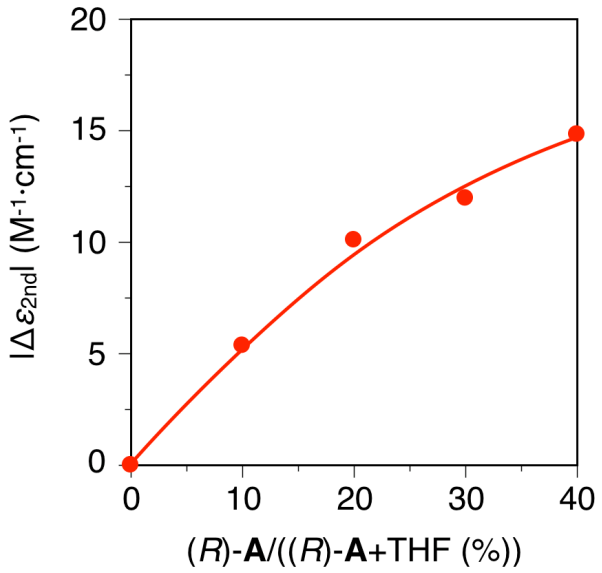

Fig. S20. CD titration curve ($|\Delta\varepsilon_{2nd}|$) of poly-**4b** with (*R*)-**A** in THF at 25 °C after standing at 25 °C for 48 h. [Poly-**4b**] = 1.0 mM.

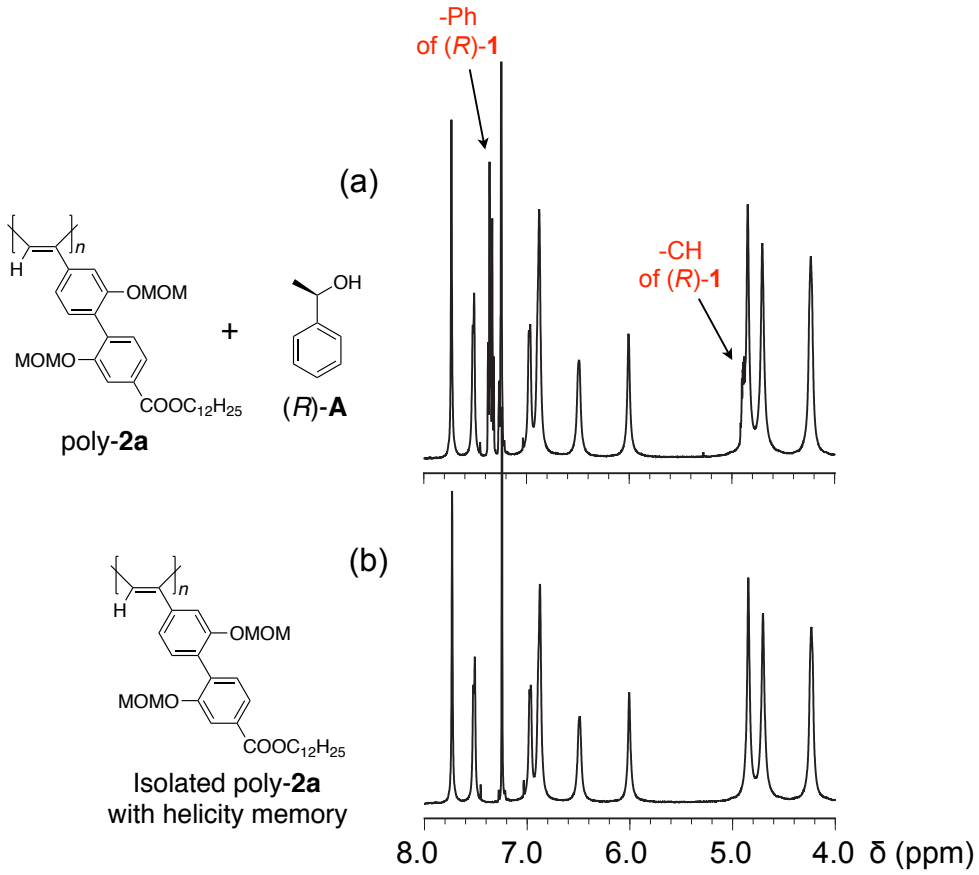

Fig. S21. ^{1}H NMR spectra of poly-**2a** with (*R*)-**A** ([(*R*)-**A**]/[poly-**2a**] = 0.3) (a) and the isolated poly-**2a** with helicity memory (b) in $CDCl_3$ at 55 °C.

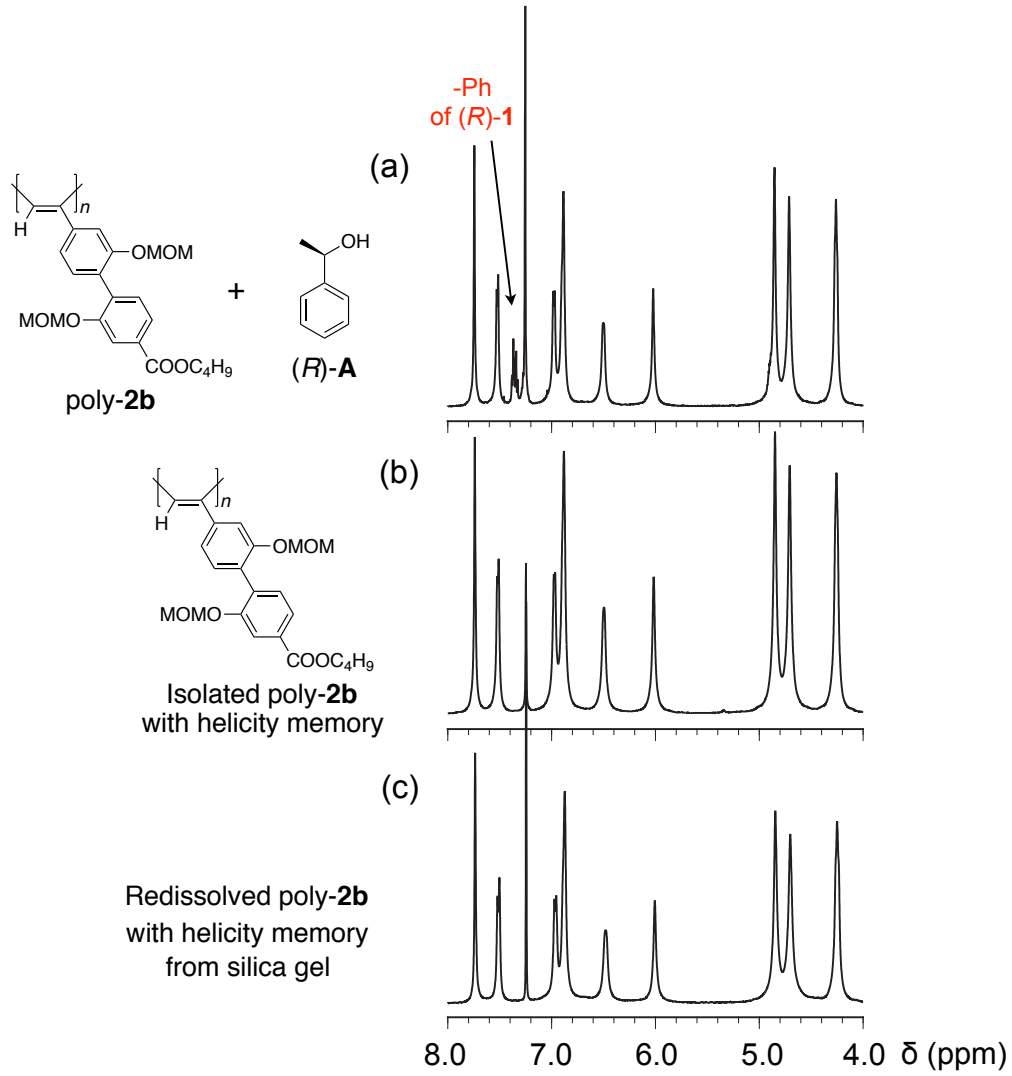

Fig. S22. ^{1}H NMR spectra of poly-**2b** with (*R*)-**A** ([(*R*)-**A**/[poly-**2a**] = 0.1] (a), the isolated poly-**2b** with helicity memory (b) and the redissolved poly-**2b** with helicity memory from silica gel (c) in $CDCl_3$ at 55 °C.

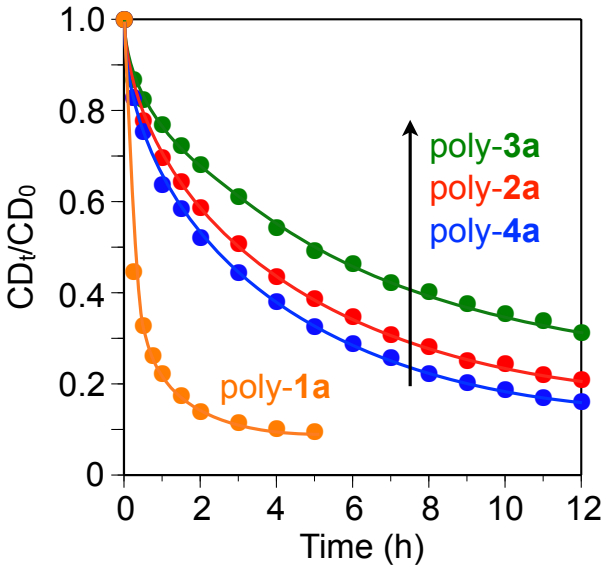

Fig. S23. Plots of the ICD intensity changes (CD_t/CD_0) of the isolated poly-**1a** (orange line), poly-**2a** (red line), poly-**3a** (green line) and poly-**4a** (blue line) in toluene at 25 °C with time. CD_0 represents the initial ICD intensity ($\Delta\varepsilon_{2nd}$) of the isolated polymers measured in toluene at –10 °C after helicity induction in toluene/(*R*)-**A** (80/20, v/v) at 25 °C for 48 h. [polymers] = 1.0 mM.

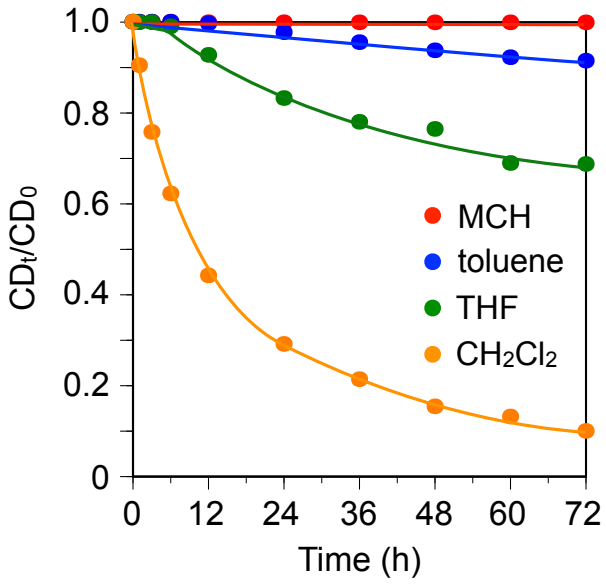

Fig. S24. Plots of the ICD intensity changes (CD_t/CD_0) of the isolated poly-**2a** at –10 °C in various solvents with time. The ICD intensity changes were estimated based on the ICD values of $\Delta\varepsilon_{2nd}$ and the CD_0 represents the initial ICD intensity of the isolated poly-**2a** in each solvent at –10 °C. [poly-**2a**] = 1.0 mM.

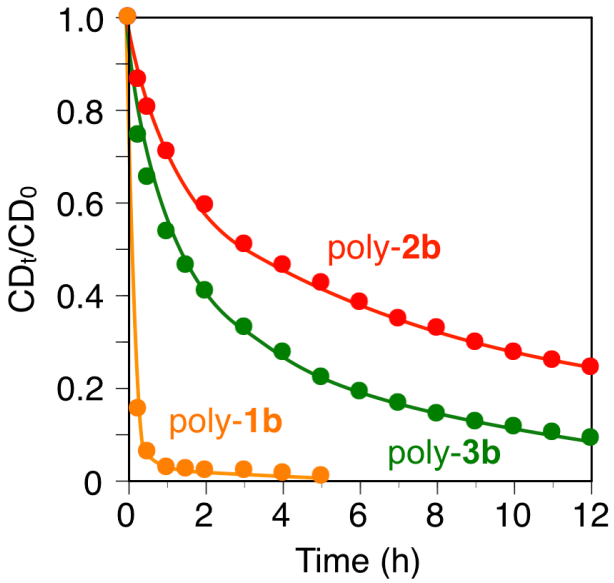

Fig. S25. Plots of the ICD intensity changes (CD_t/CD_0) of isolated poly-**1b** (orange line), poly-**2b** (red line) and poly-**3b** (green line) in toluene at 25 °C with time. CD_0 represents the initial ICD intensity of the isolated polymers in toluene at –10 °C after helicity induction in toluene/(*R*)-**A** (80/20, v/v) at 25 °C for 48 h. [Polymers] = 1.0 mM.

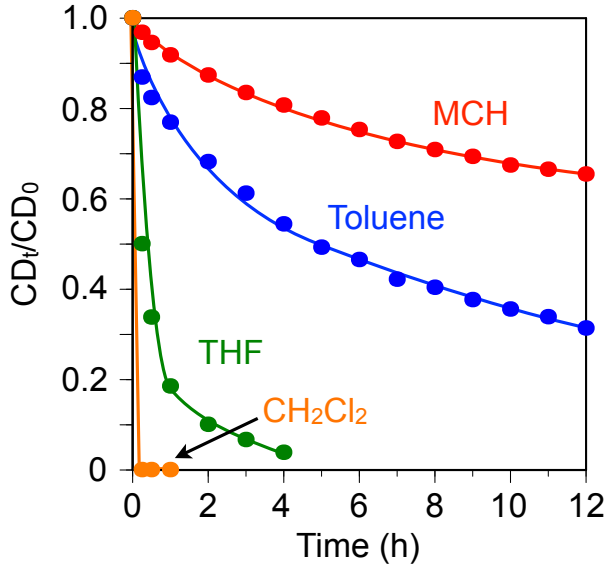

Fig. S26. Plots of the ICD intensity changes (CD_t/CD_0) of the isolated poly-**2a** at 25 °C in various solvents with time. The ICD intensity changes were estimated based on the ICD values of $\Delta\varepsilon_{2nd}$ and the CD_0 represents the initial ICD intensity of the isolated poly-**2a** in each solvent at –10 °C. [poly-**2a**] = 1.0 mM.

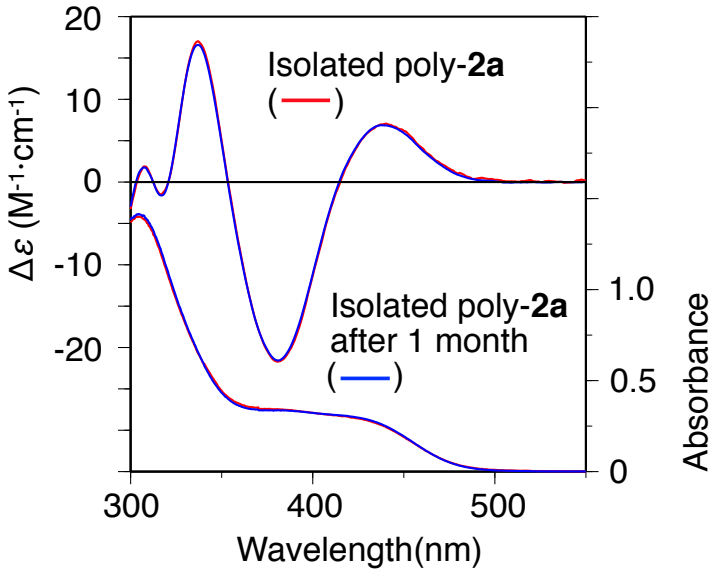

Fig. S27. CD and absorption spectra of poly-**2a** measured in toluene at –10 °C just after isolation (red lines) and those after standing at 25 °C for 1 month in the solid state (blue lines).

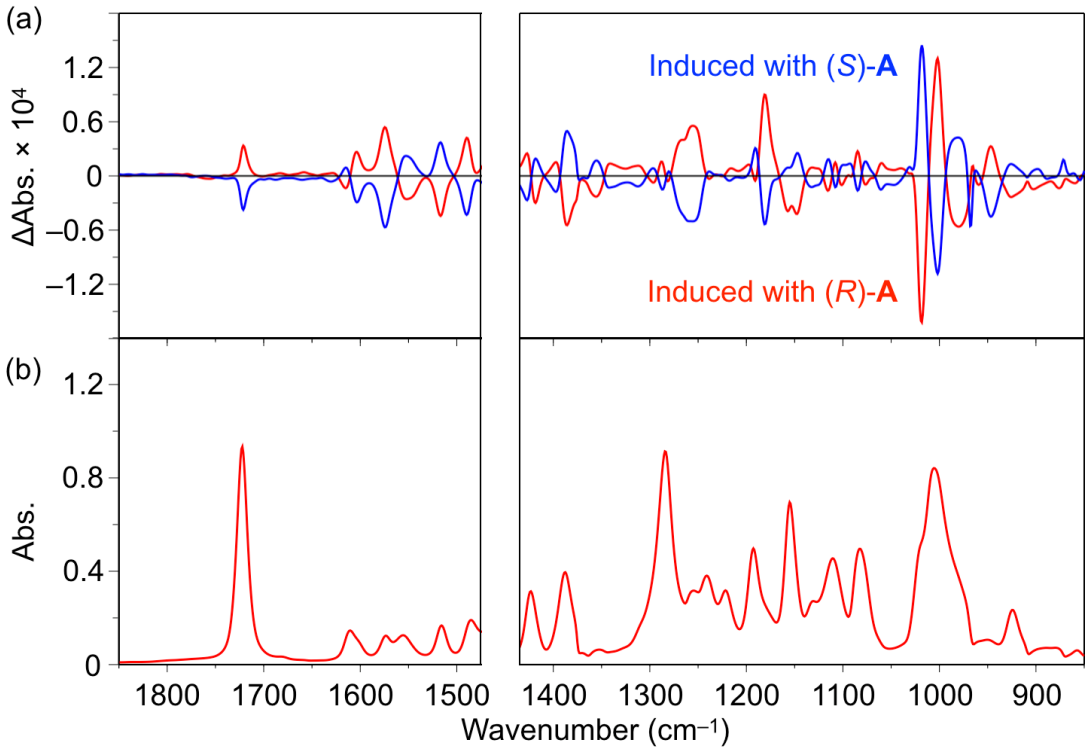

Fig. S28. (a) VCD spectra of the isolated poly-**2a** in MCH at –10 °C after helicity induction with (*R*)-**A** (red line) and (*S*)-**A** (blue line). (b) IR spectrum of the isolated poly-**2a** in MCH at –10 °C after helicity induction with (*R*)-**A** is also shown.

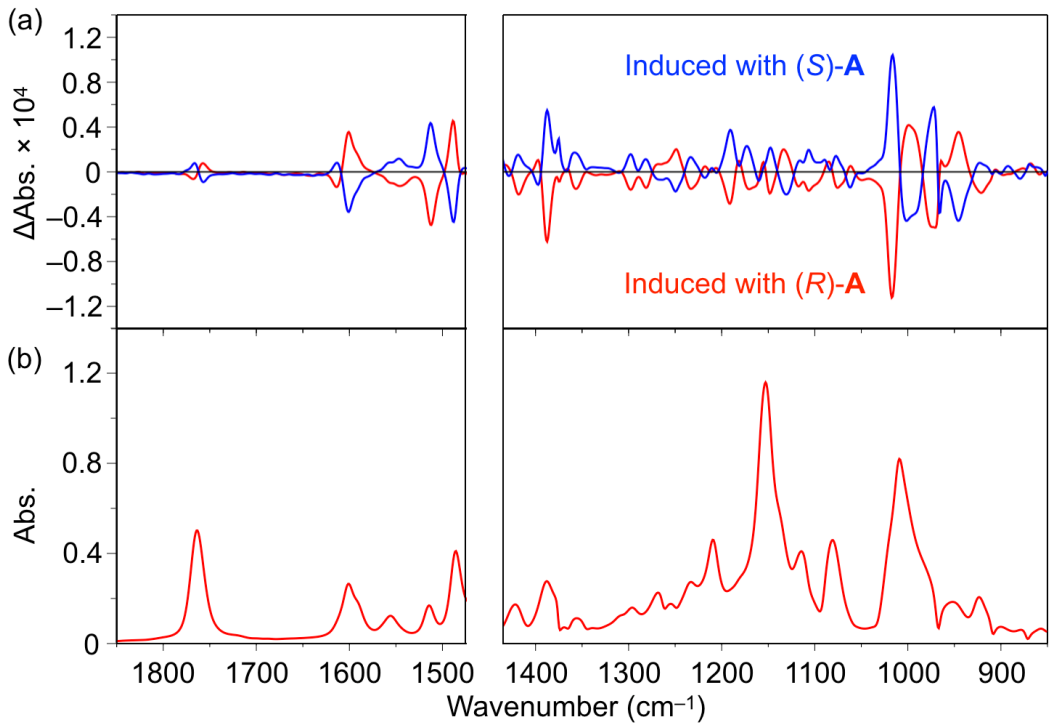

Fig. S29. (a) VCD spectra of the isolated poly-**3a** in MCH at –10 °C after helicity induction with (*R*)-**A** (red line) and (*S*)-**A** (blue line). (b) IR spectrum of the isolated poly-**3a** in MCH at –10 °C after helicity induction with (*R*)-**A** is also shown.

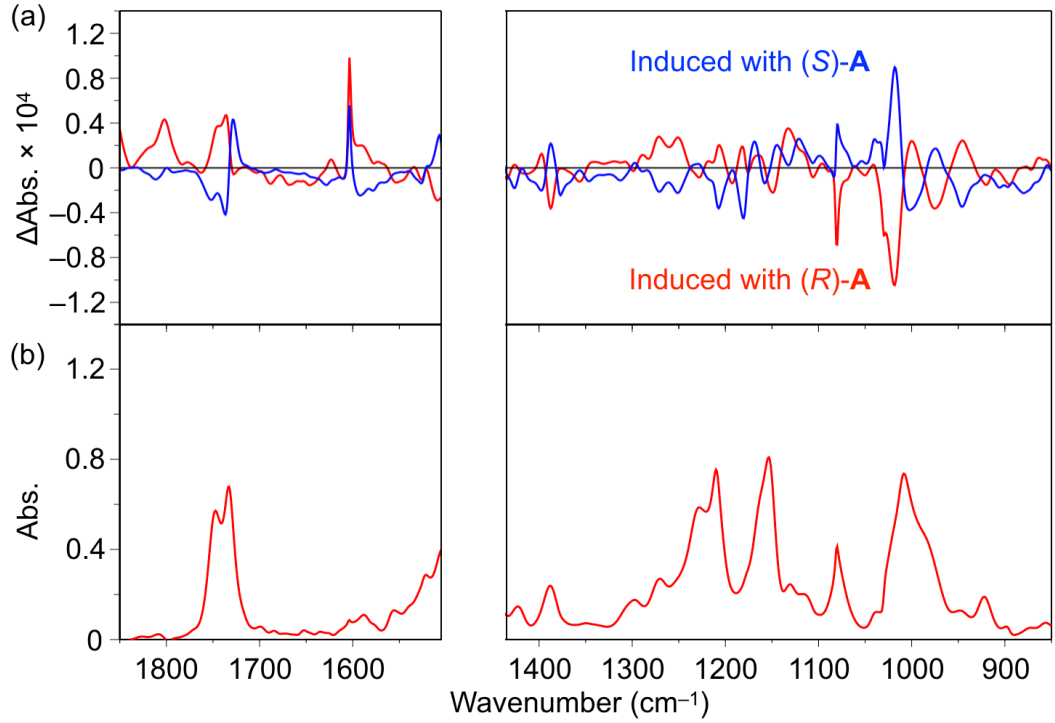

Fig. S30. (a) VCD spectra of the isolated poly-**4a** in toluene at –10 °C after helicity induction with (*R*)-**A** (red line) and (*S*)-**A** (blue line). (b) IR spectrum of the isolated poly-**4a** in toluene at –10 °C after helicity induction with (*R*)-**A** is also shown.

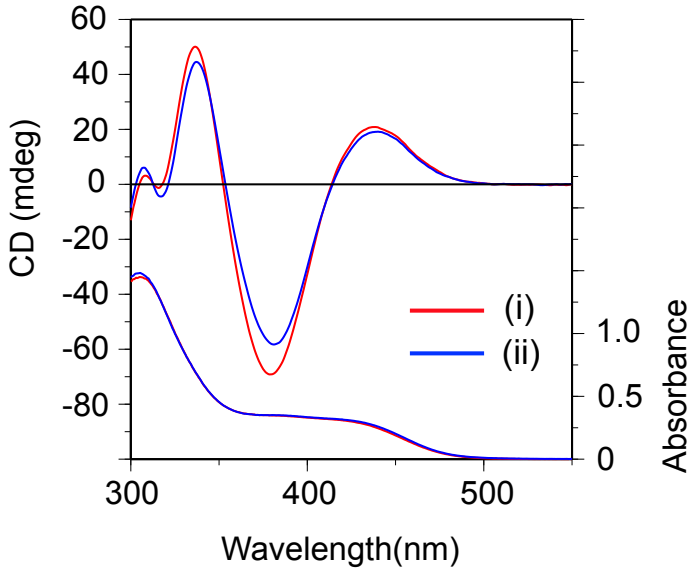

Fig. S31. CD and absorption spectra of poly-**2b** measured in toluene/(*R*)-**A** (80/20, v/v) at 25 °C after standing at 25 °C for 48 h (i) and the recovered poly-**2b** from silica surface in toluene at –10 °C (ii).

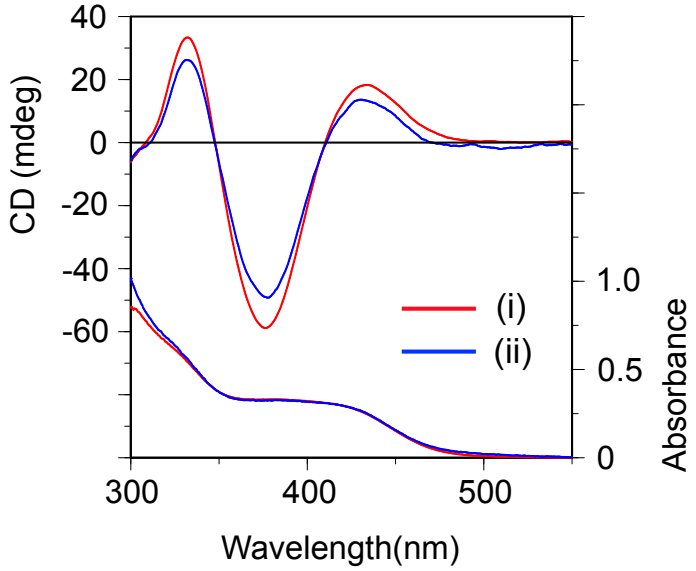

Fig. S32. CD and absorption spectra of poly-**3b** measured in toluene/(*R*)-**A** (80/20, v/v) at 25 °C after standing at 25 °C for 48 h (i) and the recovered poly-**3b** from silica surface in toluene at –10 °C (ii).

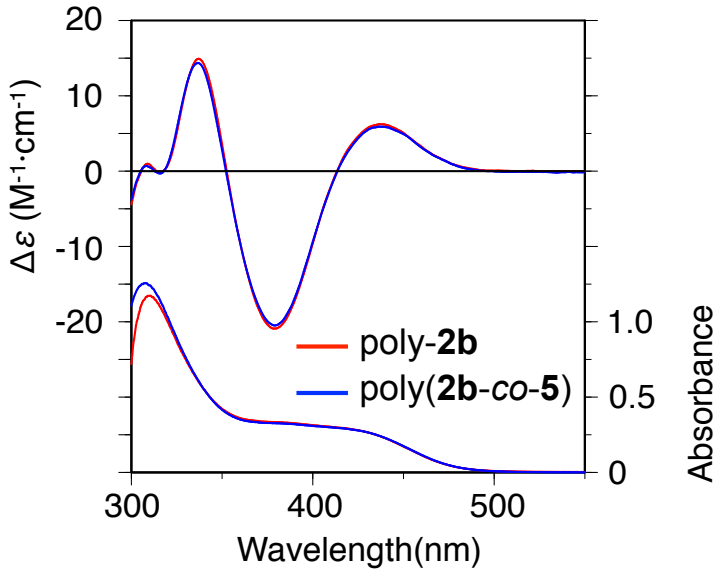

Fig. S33. CD and absorption spectra of poly-**2b** (red lines) and poly(**2b**-*co*-**5**) (blue lines) measured in toluene/(*R*)-**A** (50/50, v/v) at 25 °C after standing at 25 °C for 48 h. [Polymer] = 1.0 mM.

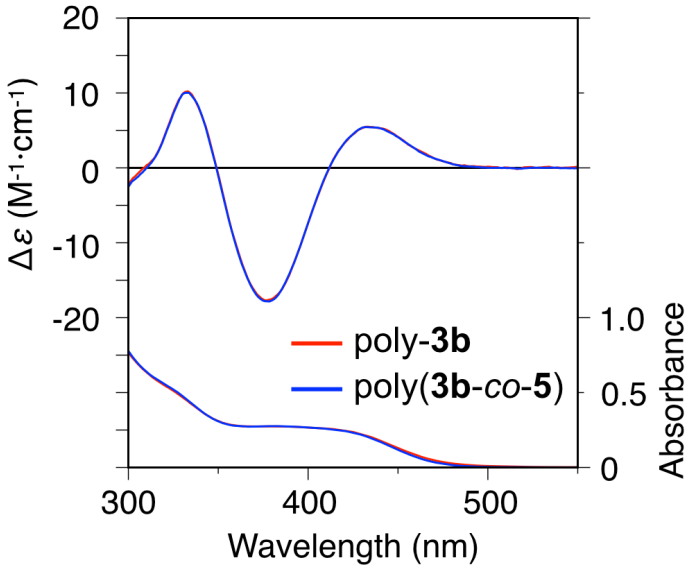

Fig. S34. CD and absorption spectra of poly-**3b** (red lines) and poly(**3b**-*co*-**5**) (blue lines) measured in toluene/(*R*)-**A** (50/50, v/v) at 25 °C after standing at 25 °C for 48 h. [Polymer] = 1.0 mM.

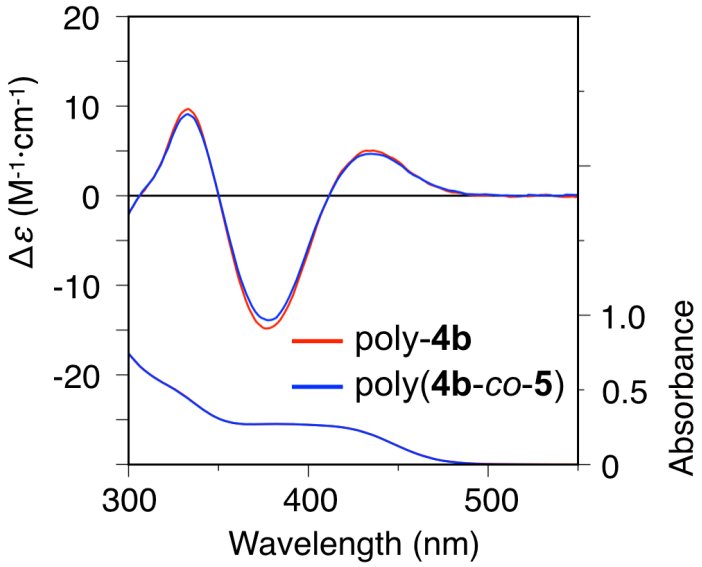

Fig. S35. CD and absorption spectra of poly-**4b** (red lines) and poly(**4b**-*co*-**5**) (blue lines) measured in THF/(*R*)-**A** (60/40, v/v) at 25 °C after standing at 25 °C for 48 h. [Polymer] = 1.0 mM.

Table S2. Resolution results of racemates **E**, **I** and **J** on Si-poly(**2b**-*co*-**5**)-based CSP

racemates	*P*-Si-poly(**2b**-*co*-**5**) (induced by (*R*)-**A**)		*M*-Si-poly(**2b**-*co*-**5**) (induced by (*S*)-**A**)		*P′*-Si-poly(**2b**-*co*-**5**) (induced by (*R*)-**A**)	
	k_1	α	k_1	α	k_1	α
E	2.67	1.06 (+)	2.61	1.05 (–)	2.46	1.06 (+)
I	0.57	1.11 (–)	0.57	1.11 (+)	0.57	1.10 (–)
J	0.81	1.14 (–)	0.80	1.14 (+)	0.80	1.14 (–)

Column: 25 x 0.20 (i.d.) cm; eluent: *n*-hexane–2-propanol (97/3, v/v); flow rate: 0.2 mL/min. The signs in parentheses represent the Cotton effect signs at 254 nm of the first-eluted enantiomers.

Table S3. Resolution results of racemates **C** and **D** on Si-poly(**3b**-*co*-**5**)-based CSP

racemates	*P*-Si-poly(**3b**-*co*-**5**) (induced by (*R*)-**A**)		*M*-Si-poly(**3b**-*co*-**5**) (induced by (*S*)-**A**)		*P′*-Si-poly(**3b**-*co*-**5**) (induced by (*R*)-**A**)	
	k_1	α	k_1	α	k_1	α
C	6.00	1.07 (–)	6.08	1.07 (+)	6.16	1.07 (–)
D	3.34	1.12 (–)	3.31	1.13 (+)	3.29	1.13 (–)

Column: 25 x 0.20 (i.d.) cm; eluent: *n*-hexane–2-propanol (97/3, v/v); flow rate: 0.2 mL/min. The signs in parentheses represent the Cotton effect signs at 254 nm of the first-eluted enantiomers.

Table S4. Resolution results of racemates **D**, **E** and **H** on Si-poly(**4b**-*co*-**5**)-based CSP

racemates	*P*-Si-poly(**4b**-*co*-**5**) (induced by (*R*)-**A**)		*M*-Si-poly(**4b**-*co*-**5**) (induced by (*S*)-**A**)		*P′*-Si-poly(**4b**-*co*-**5**) (induced by (*R*)-**A**)	
	k_1	α	k_1	α	k_1	α
D	2.08	1.35 (–)	2.06	1.34 (+)	2.13	1.34 (–)
E	5.30	1.08 (+)	4.92	1.07 (–)	5.06	1.07 (+)
H	3.21	1.08 (–)	3.22	1.06 (+)	3.35	1.06 (–)

Column: 25 x 0.20 (i.d.) cm; eluent: *n*-hexane–2-propanol (97/3, v/v); flow rate: 0.2 mL/min. The signs in parentheses represent the Cotton effect signs at 254 nm of the first-eluted enantiomers.

10. ^{1}H and ^{13}C NMR spectra of monomers and polymers

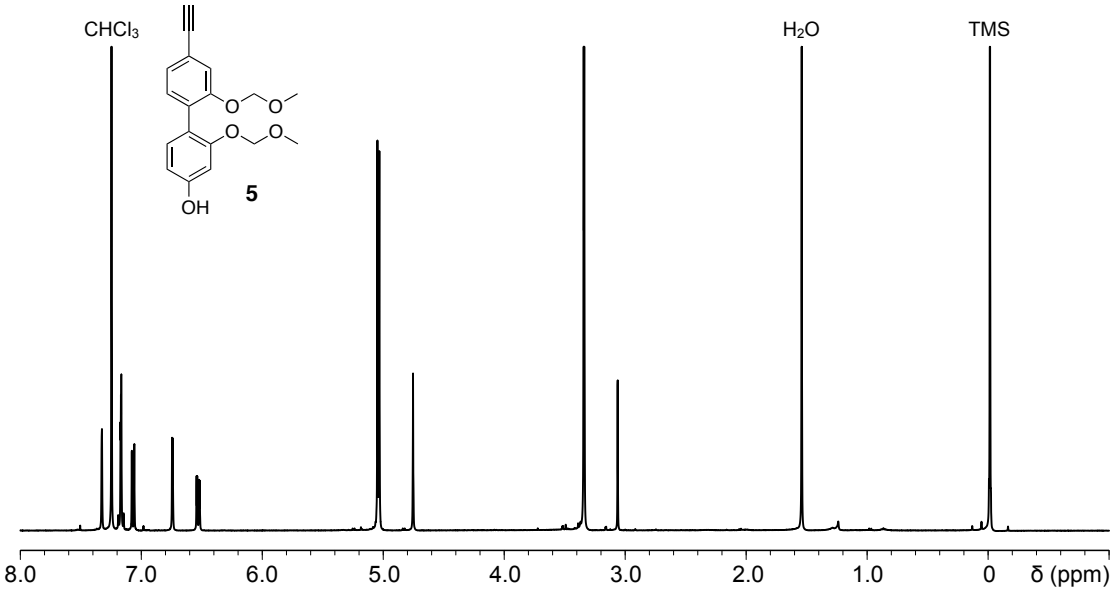

Fig. S36. ^{1}H NMR spectrum of **5** in $CDCl_3$ at 25 °C.

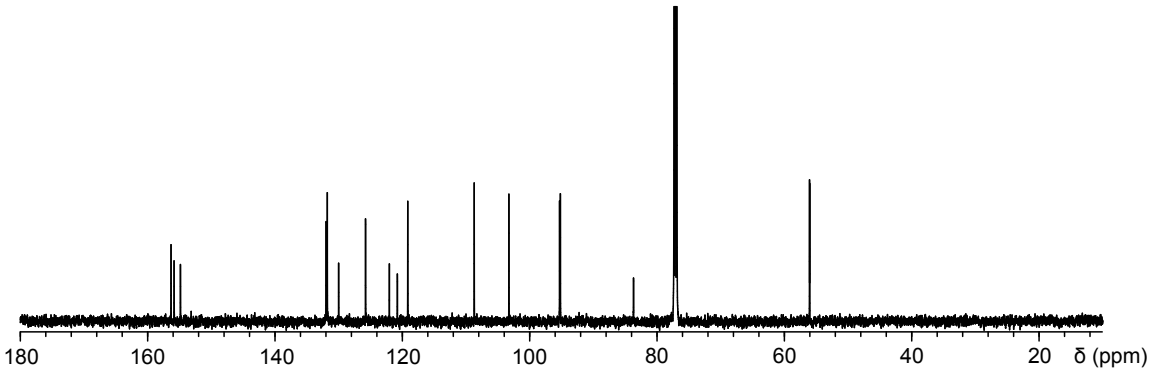

Fig. S37. ^{13}C NMR spectrum of **5** in $CDCl_3$ at 25 °C.

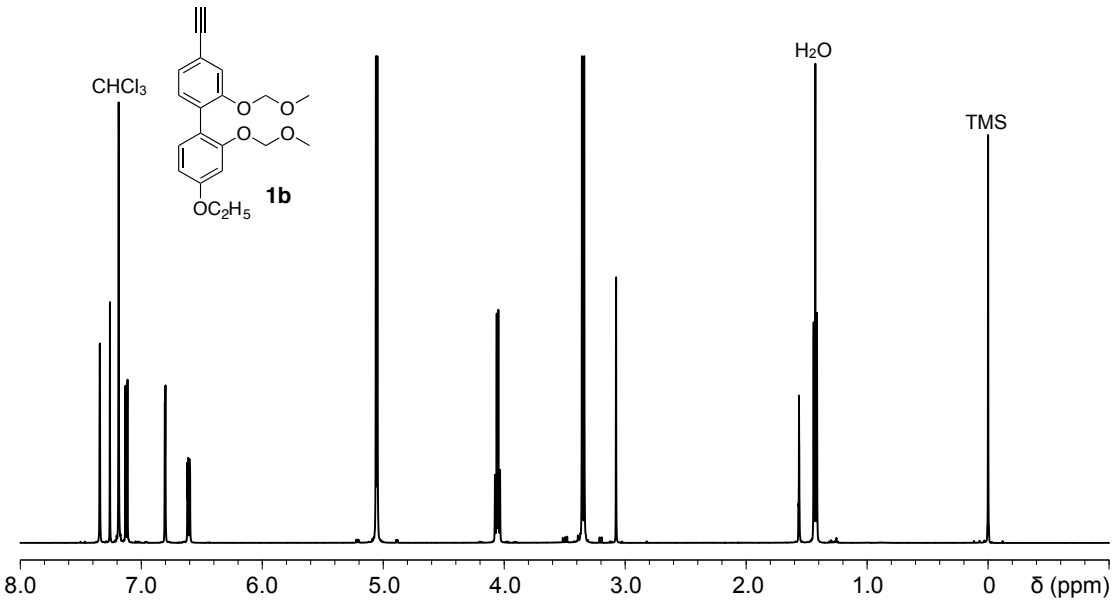

Fig. S38. ^{1}H NMR spectrum of **1b** in $CDCl_3$ at 25 °C.

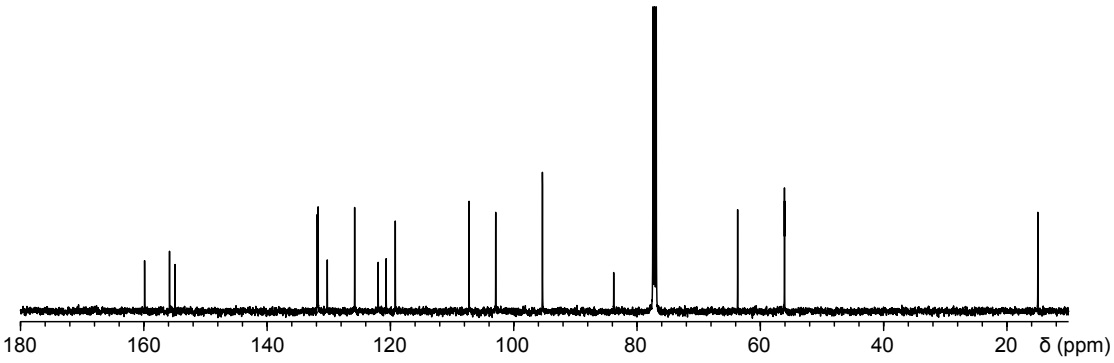

Fig. S39. ^{13}C NMR spectrum of **1b** in $CDCl_3$ at 25 °C.

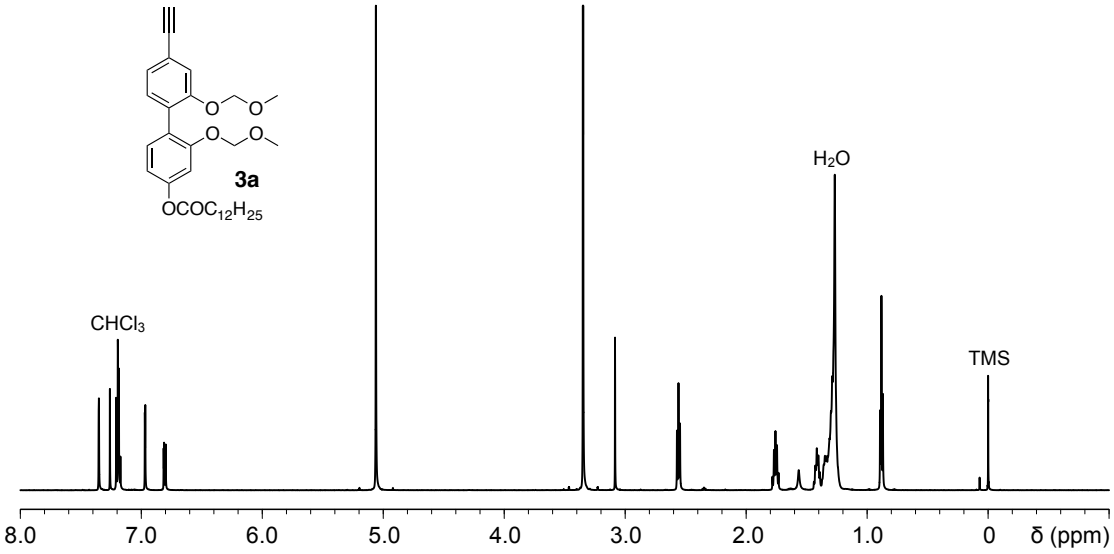

Fig. S40. ^{1}H NMR spectrum of **3a** in $CDCl_3$ at 25 °C.

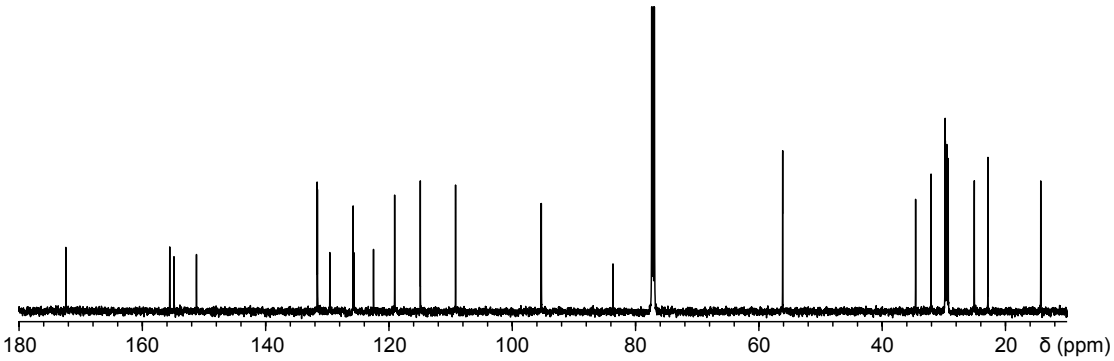

Fig. S41. ^{13}C NMR spectrum of **3a** in $CDCl_3$ at 25 °C.

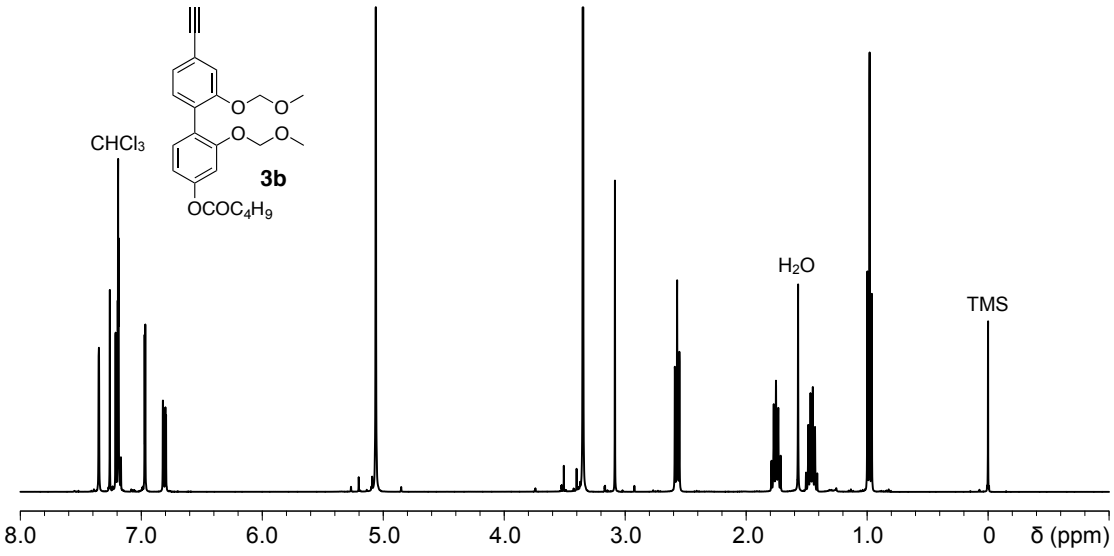

Fig. S42. ^{1}H NMR spectrum of **3b** in $CDCl_3$ at 25 °C.

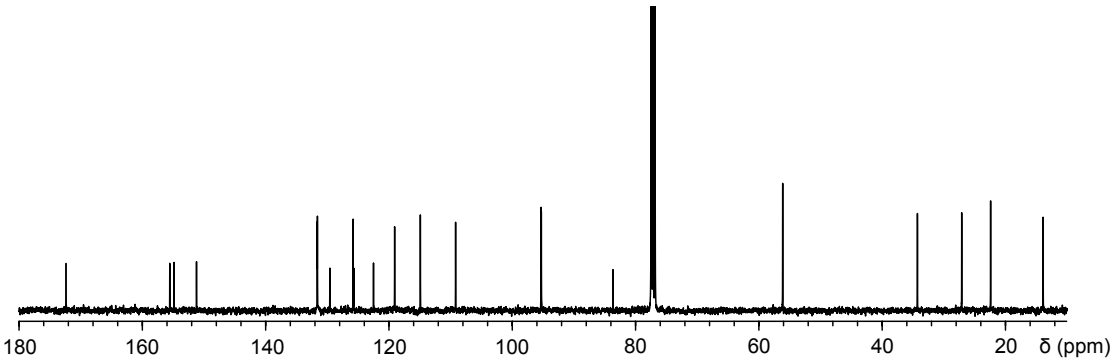

Fig. S43. ^{13}C NMR spectrum of **3b** in $CDCl_3$ at 25 °C.

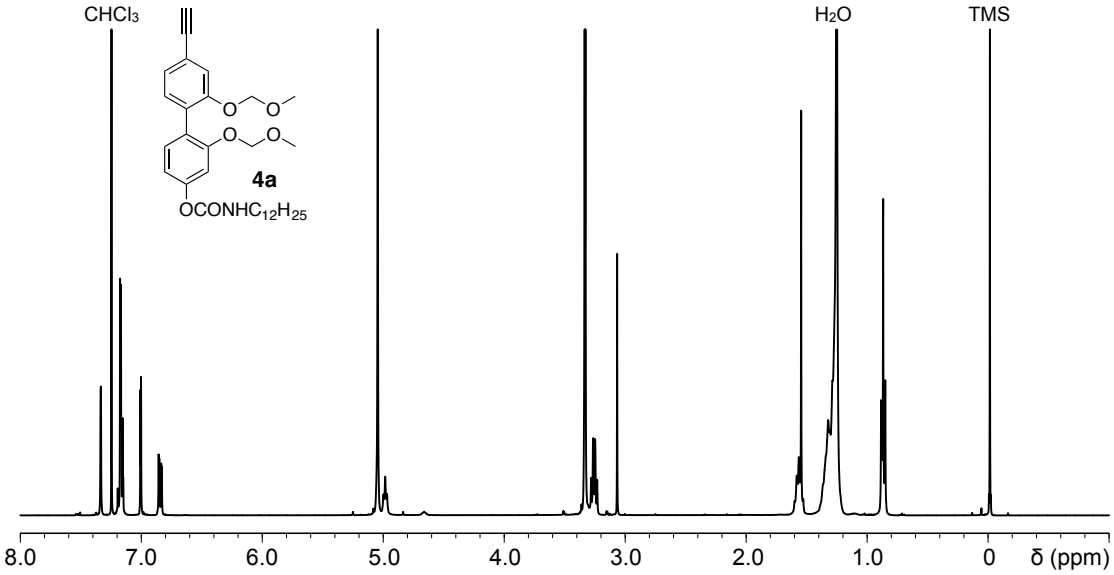

Fig. S44. ^{1}H NMR spectrum of **4a** in $CDCl_3$ at 25 °C.

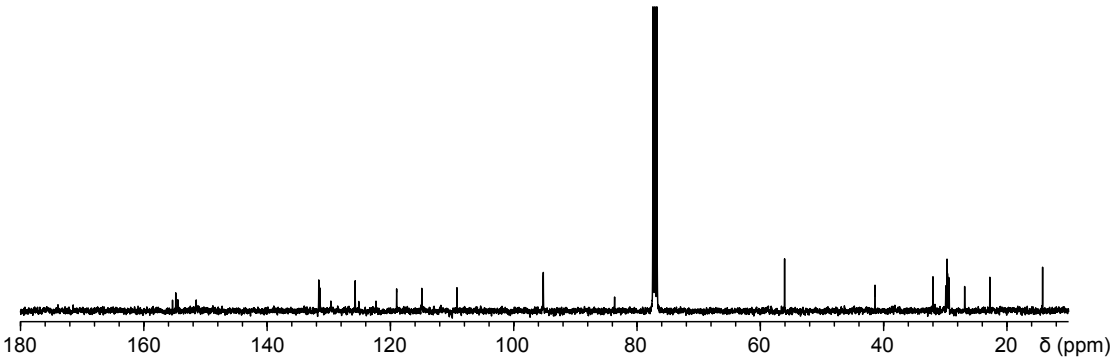

Fig. S45. ^{13}C NMR spectrum of **4a** in $CDCl_3$ at 25 °C.

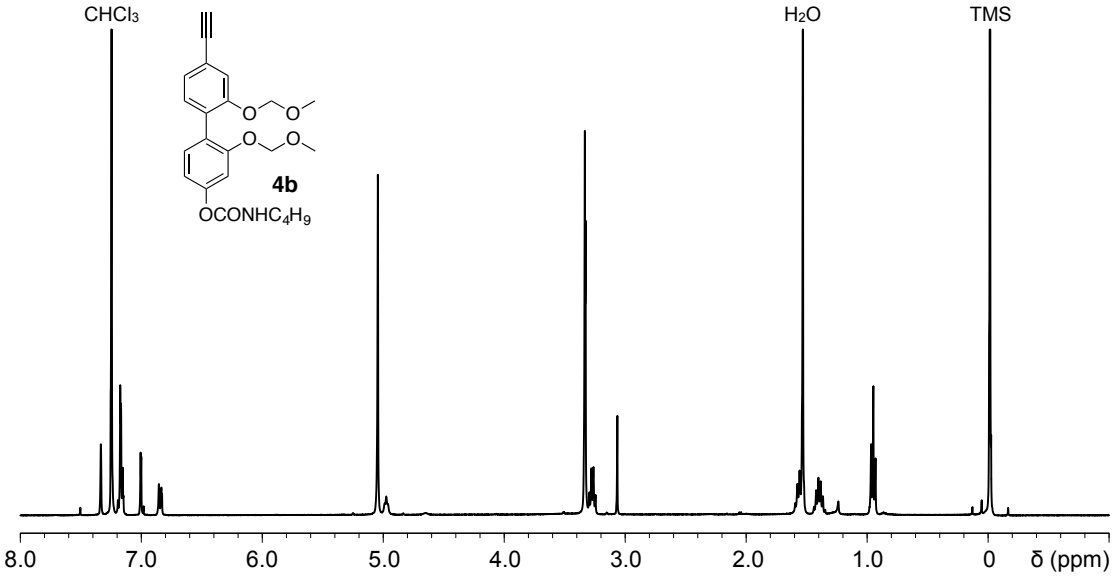

Fig. S46. ^{1}H NMR spectrum of **4b** in $CDCl_3$ at 25 °C.

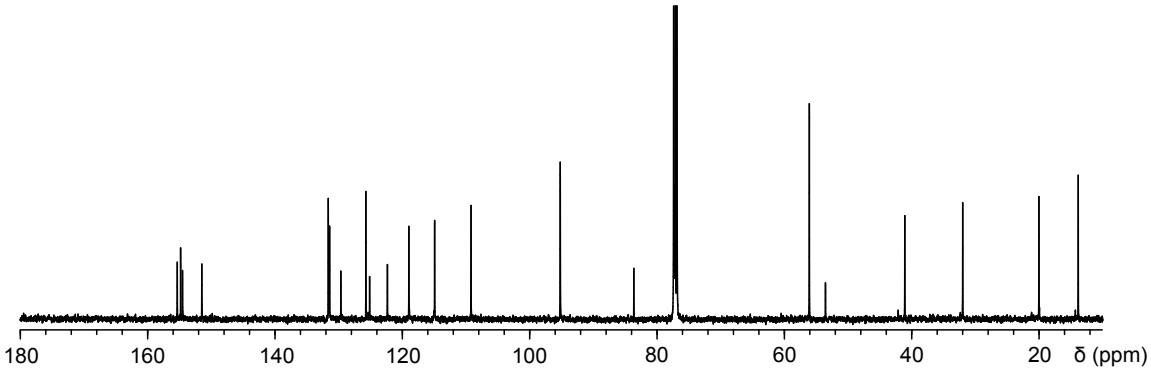

Fig. S47. ^{13}C NMR spectrum of **4b** in $CDCl_3$ at 25 °C.

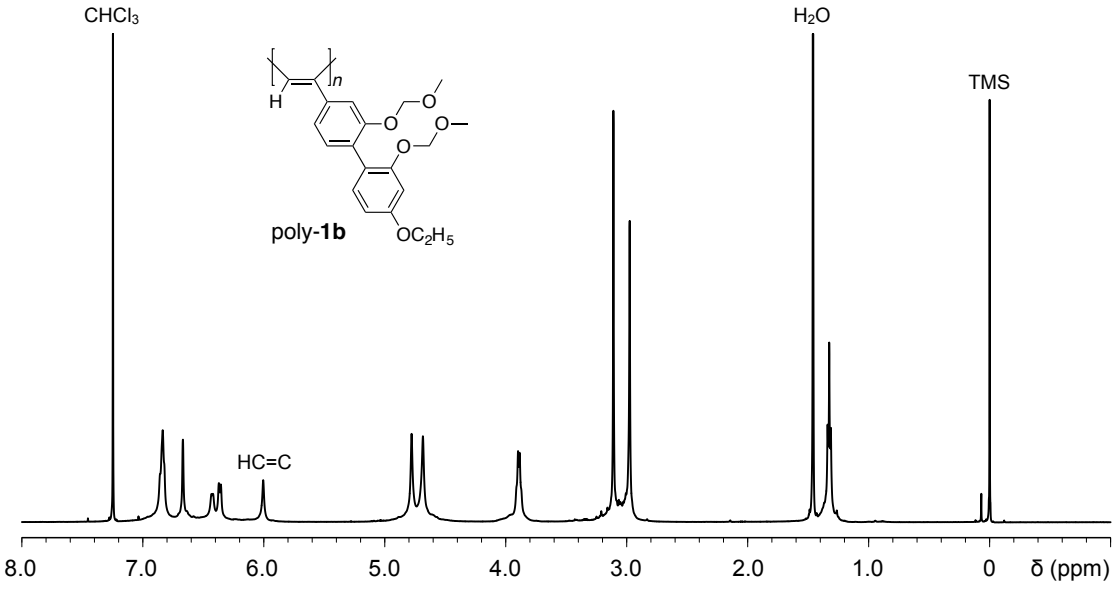

Fig. S48. ^{1}H NMR spectrum of poly-**1b** in $CDCl_3$ at 55 °C.

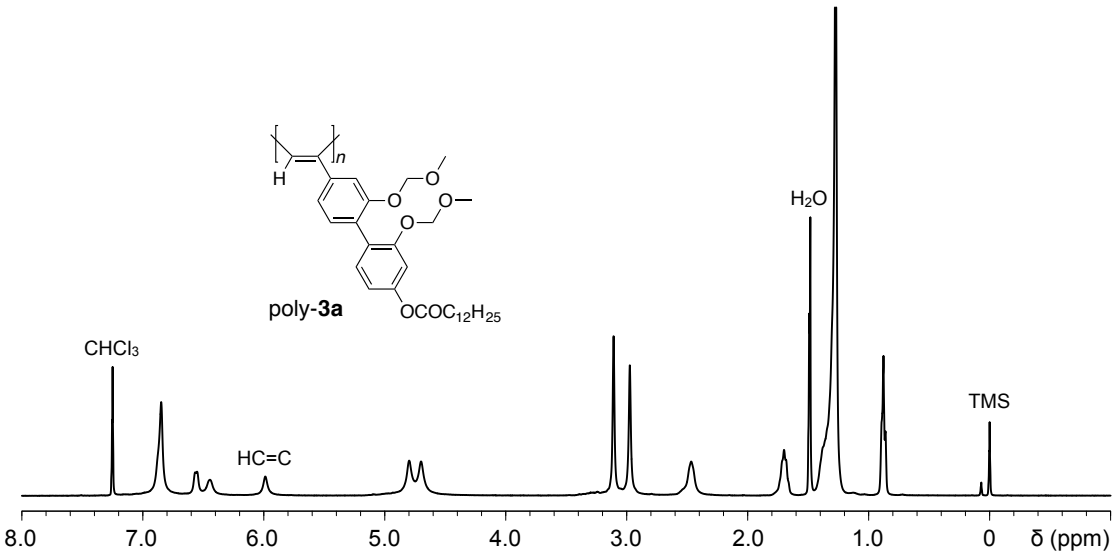

Fig. S49. ^{1}H NMR spectrum of poly-**3a** in $CDCl_3$ at 55 °C.

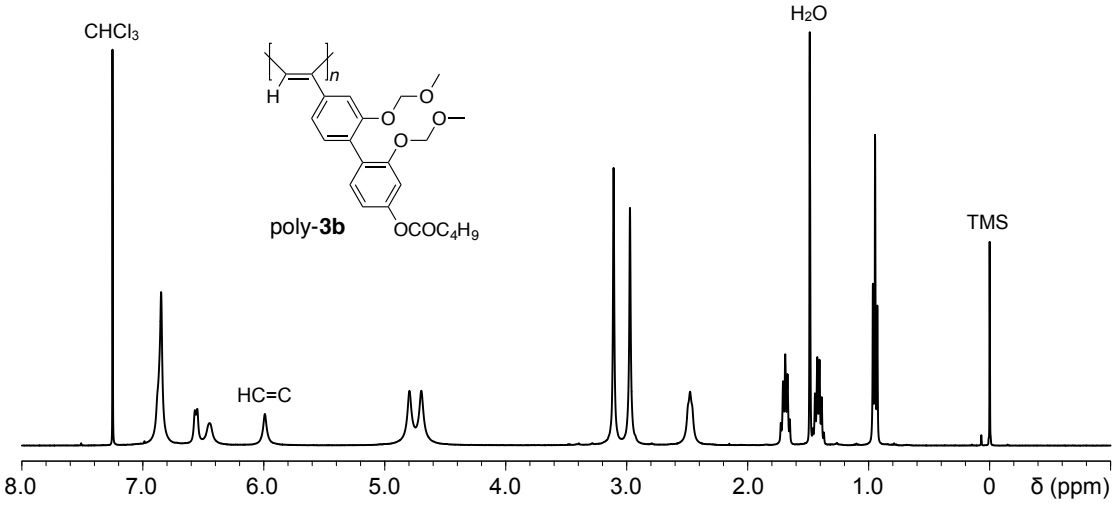

Fig. S50. ^{1}H NMR spectrum of poly-**3b** in $CDCl_3$ at 55 °C.

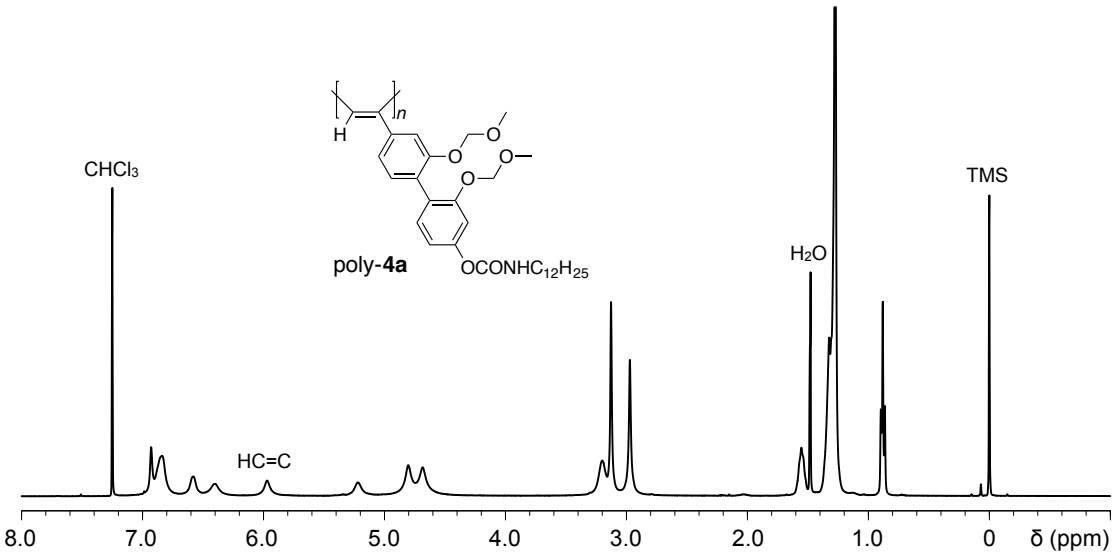

Fig. S51. ^{1}H NMR spectrum of poly-**4a** in $CDCl_3$ at 55 °C.

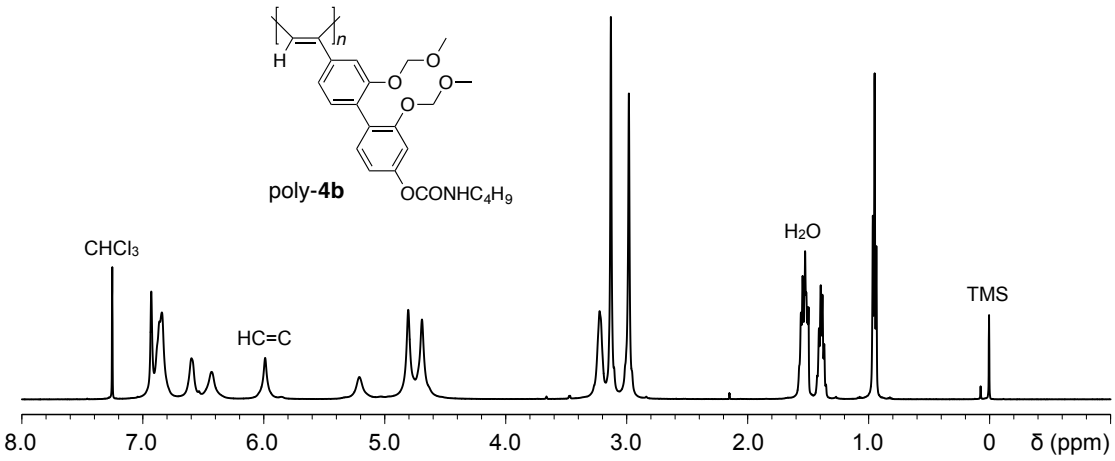

Fig. S52. ^{1}H NMR spectrum of poly-**4b** in $CDCl_3$ at 55 °C.

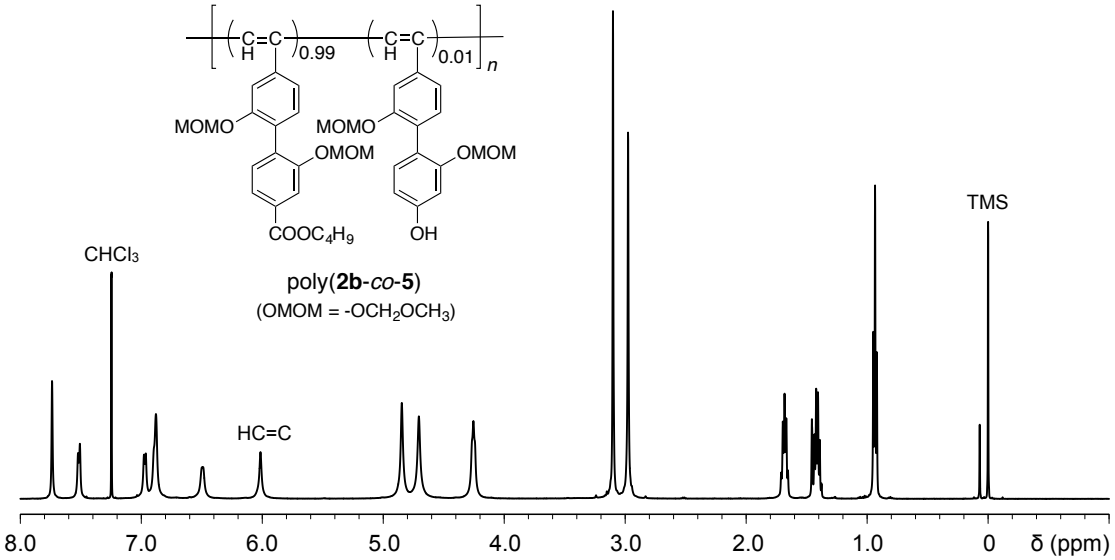

Fig. S53. ^{1}H NMR spectrum of poly(**2b**-*co*-**5**) in $CDCl_3$ at 55 °C.

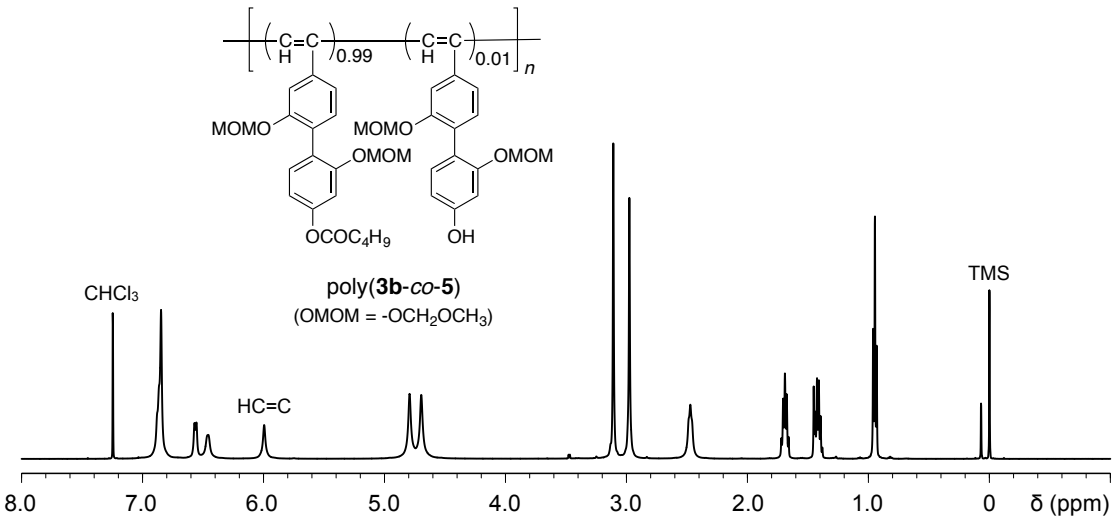

Fig. S54. ^{1}H NMR spectrum of poly(**3b**-*co*-**5**) in $CDCl_3$ at 55 °C.

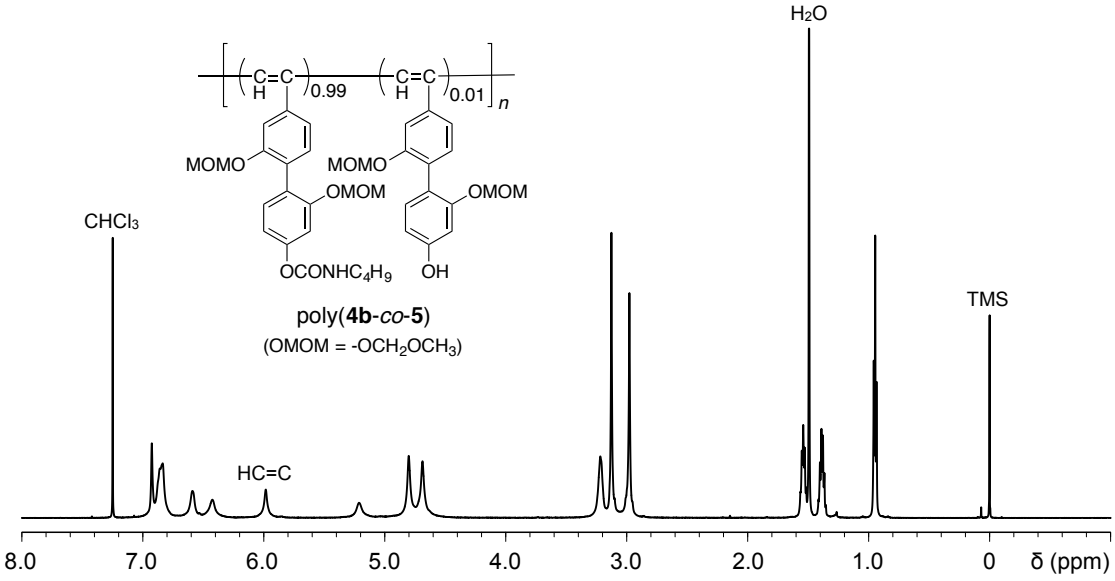

Fig. S55. ^{1}H NMR spectrum of poly(**4b**-*co*-**5**) in $CDCl_3$ at 55 °C.

11. Supporting references

S1. K. Maeda, D. Hirose, N. Okoshi, K. Shimomura, Y. Wada, T. Ikai, S. Kanoh and E. Yashima, *J. Am. Chem. Soc.*, 2018, **140**, 3270-3276.

S2. R. Ishidate, T. Ikai, S. Kanoh, E. Yashima and K. Maeda, *Chirality*, 2017, **29**, 120-129.

S3. R. Ishidate, K. Shimomura, T. Ikai, S. Kanoh and K. Maeda, *Chem. Lett.*, 2015, **44**, 946-948.

S4. K. Shimomura, T. Ikai, S. Kanoh, E. Yashima and K. Maeda, *Nat. Chem.*, 2014, **6**, 429-434.

S5. Y. Okamoto, R. Aburatani and K. Hatada, *J. Chromatogr.*, 1987, **389**, 95-102.

S6. Y. Okamoto, M. Kawashima and K. Hatada, *J. Chromatogr.*, 1986, **363**, 173-186.

S7. H. Koller, K.-H. Rimböck and A. Mannschreck, *J. Chromatogr. A*, 1983, **282**, 89-94.